Acta Crystallographica Section A
Foundations of Crystallography
ISSN 0108-7673

Received 19 April 2010
Accepted 21 October 2010

Euclidian embeddings of periodic nets: definition of a topologically induced complete set of geometric descriptors for crystal structures

Jean-Guillaume Eon

Instituto de Química, Universidade Federal do Rio de Janeiro, Avenida Athos da Silveira Ramos, 149 Bloco A, Cidade Universitária, Rio de Janeiro 21941-909, Brazil. Correspondence e-mail: jgeon@iq.ufrj.br

Crystal-structure topologies, represented by periodic nets, are described by labelled quotient graphs (or voltage graphs). Because the edge space of a finite graph is the direct sum of its cycle and co-cycle spaces, a Euclidian representation of the derived periodic net is provided by mapping a basis of the cycle and co-cycle spaces to a set of real vectors. The mapping is consistent if every cycle of the basis is mapped on its own net voltage. The sum of all outgoing edges at every vertex may be chosen as a generating set of the co-cycle space. The embedding maps the cycle space onto the lattice L. By analogy, the concept of the *co-lattice* L^* is defined as the image of the generators of the co-cycle space; a co-lattice vector is proportional to the distance vector between an atom and the centre of gravity of its neighbours. The pair (L, L^*) forms a complete geometric descriptor of the embedding, generalizing the concept of barycentric embedding. An algebraic expression permits the direct calculation of fractional coordinates. Non-zero co-lattice vectors allow nets with collisions, displacive transitions *etc.* to be dealt with. The method applies to nets of any periodicity and dimension, be they crystallographic nets or not. Examples are analyzed: α-cristobalite, the seven unstable 3-periodic minimal nets *etc.*

1. Introduction

After the pioneering works of Wells (1977) and O'Keeffe & Hyde (1980), 2- or 3-periodic nets have been commonly used to describe the topology of crystal structures. General definitions and recent developments in the application of graph theory to crystal chemistry have been summarized by Delgado-Friedrichs & O'Keeffe (2005) and Delgado-Friedrichs *et al.* (2005). Periodic nets are infinite graphs and it is convenient to handle their quotient graph in relation to a maximal translation subgroup, since the latter is a finite graph. Labelled quotient graphs are particularly more suitable because they are in a one-to-one correspondence with periodic nets (Chung *et al.*, 1984; Delgado-Friedrichs, 2004). It is easily verified that the space group of a crystal structure is isomorphic to a subgroup of the automorphism group of the associated net. In this work we turn back to the converse problem of finding a Euclidian embedding (*i.e.* an injective representation) of maximum acceptable symmetry for a p-periodic net, given its labelled quotient graph. This problem is significant in the context of systematic generation of periodic nets derived from pre-defined classes of labelled quotient graphs. We look then for an embedding of the derived periodic net whose space group is both maximal in the full combinatorial automorphism group of the net and consistent with the given quotient graph.

Delgado-Friedrichs & O'Keeffe (2003) and Delgado-Friedrichs (2004, 2005) defined *equilibrium* or *barycentric placements* of periodic graphs in Euclidian space as realizations of the graph where each vertex is at the centre of gravity of its neighbours. It was shown that (i) equilibrium placements are essentially unique and (ii) every *periodic automorphism* (*i.e.* an automorphism which is consistent with the translation subgroup) of a periodic graph can be associated with an isometry in the equilibrium placement. The program *SYSTRE* (Delgado-Friedrichs & O'Keeffe, 2003) directly solves the linear system associated with equilibrium placements and finds the vertex coordinates and the ideal space group for 2- and 3-periodic nets without collisions. Fractional coordinates and lattice parameters may be refined within the ideal space group by minimizing the edge-length variance and maximizing the unit-cell volume, so that equilibrium placements are but convenient intermediates for finding physically more realistic embeddings.

Recently, Thimm (2009) showed that the topology of a periodic net represented by its labelled quotient graph determines the minimal (inevitable) symmetry as well as the maximal possible symmetry of an embedding. The analysis

uses the linear representation of the automorphisms of the quotient graph that are consistent with the vector labels. This technique was already described in previous works (Eon, 1998; Klee, 2004; Thimm & Winkler, 2006) and enables the constraints on edge vectors imposed by the existence of some symmetry operation to be written down.

Although they are complementary in some sense, both cited approaches miss some relevant inter-relationship between topology and geometry, specifically site symmetry. In the approach of the equilibrium placement, the embedding must be found before the respective space group is determined. It is known (Delgado-Friedrichs *et al.*, 2005) that descent in symmetry may be necessary in some cases, as for nets with collisions, but no general technique seems to have been reported, at least to the knowledge of this author. In contrast, descent in symmetry is allowed in Thimm's approach but structural motives remain hidden: why should one look for lower symmetry and how much lower? In both cases site symmetry is casually read off from final data. This paper describes a unifying graph-theoretical framework for the construction of Euclidian embeddings of periodic nets with the maximum acceptable symmetry. The determinant role of site symmetry (local distortions) as structure-directing in conjunction with topology is emphasized. Two complementary points of view are integrated here.

(1) A periodic net N with quotient graph G is isomorphic to a (partial) quotient of the minimal net $M(G)$ derived from G. This property has geometrical implications: it is possible to obtain a representation of the net N as a projection of an embedding of the minimal net $M(G)$. Several examples were examined by Eon (1998).

(2) Because the cycle and co-cycle spaces of a finite graph are supplementary vector spaces with respect to its edge space, a Euclidian representation of the derived periodic net can be equivalently provided (i) by mapping the edges of the graph to a consistent set of real vectors, as performed by Thimm (2009), or (ii) by mapping the bases of the cycle and co-cycle spaces to lattice vectors and to an arbitrary set of real vectors, respectively. The latter ideas were introduced by Eon (1999).

In this contribution, embeddings are constructed according to item (2-ii), hence mapping directly the cycle space of the quotient graph onto the lattice L. By analogy, a *co-lattice* L^* is defined as the image set of the generators of the co-cycle space. The pair (L, L^*) forms a complete geometric descriptor of the embedding. The space group of the embedding defined by (L, L^*) contains only the symmetry operations of the barycentric embedding $(L, 0)$ that leave the co-lattice L^* invariant. In general, the lattice type may be determined from some barycentric representation of maximum symmetry: the construction of a particular embedding is described according to item (1), from which a metric tensor is easily determined. Non-zero co-lattice vectors may then be introduced in the case of representations with collisions or to take account of displacive transitions, for example. The method applies to nets of any periodicity and dimension, be they crystallographic nets or not. Since the goal of this paper is to describe the method, only embeddings of known periodic nets will be analyzed for illustration.

§2 gives an overview of the methodology used in the paper, with the aim of guiding the reader throughout the paper but also to justify the mathematical apparatus. The basic concepts of graph theory can be found in Harary (1972). However, we shall find it useful to cast the problem into the language of topological graph theory (Gross & Tucker, 2001), borrowing also some tools from algebraic graph theory (Godsil & Royle, 2004). Accordingly, §3 introduces the basic definitions leading to the concept of a voltage graph, which generalizes that of a labelled quotient graph. The definitions of periodic net, barycentric representation and embedding of a periodic net are given in §4, §5 and §6, respectively. The isomorphism theorem is exposed in §7. The analysis of the embedding of some 2-, 3- and 4-periodic crystallographic nets without collisions, chosen as examples for their simplicity, is presented in §8. §9 discusses two non-barycentric embeddings of stable nets, one with ideal symmetry (β-W), the other with descent in symmetry (α-cristobalite). §10 proposes maximum-symmetry embeddings for the seven unstable 3-periodic minimal nets, and §11 illustrates an application to non-crystallographic nets.

2. An overview of the methodology

This section presents a simple illustration for each of the two above-mentioned viewpoints.

2.1. Embeddings as projections

We consider here **hxl** [or (3^6), the well known triangular net], with quotient graph $\mathcal{B}_3$, the graph (*bouquet*) with one vertex and three loops, as drawn in Fig. 1. [When possible we shall name the net by using its three-letter code, as defined by O'Keeffe *et al.* (2008).]

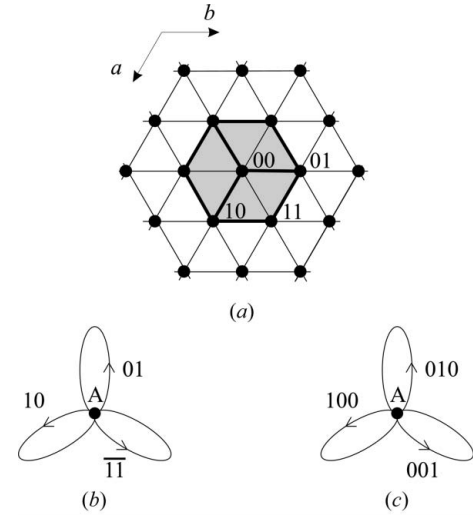

Figure 1
(*a*) The triangular net **hxl**, (*b*) its labelled quotient graph $\mathcal{B}_3$ with voltage assignment in $\mathbb{Z}^2$ and (*c*) the labelled quotient graph $\mathcal{B}_3$ of the cubic net with voltage assignment in $\mathbb{Z}^3$. The relationship between **hxl** and the unit cell of **pcu** is highlighted in (*a*).

Of course, $\mathcal{B}_3$ is also the quotient graph of the *minimal net* **pcu** (the primitive cubic net). It results that **hxl** is a quotient graph of **pcu**, which may be explicitly determined by an analysis of the essential rings of the net. We recall first that a *strong ring* is a cycle that is not the sum of any number of shorter cycles. For instance, the 4-cycle $A_{00}A_{10}A_{11}A_{01}A_{00}$ (denoting by A_{ij} the vertices of **hxl**) is the sum of two cycles: $A_{00}A_{10}A_{11}A_{00}$ and $A_{00}A_{11}A_{01}A_{00}$, which are strong rings. *Essential rings* are those strong rings which are the faces of a tiling of the embedding (Delgado-Friedrichs & O'Keeffe, 2005). The essential rings of **hxl** are the above-mentioned triangles running along three translationally non-equivalent edges of the net; in fact the two triangles tiling the unit cell determine symmetry-related strong rings and differ only in the sequence of the edges from different edge lattices. Because each edge lattice of **hxl** is represented by a loop in its quotient graph $\mathcal{B}_3$, the essential ring $A_{00}A_{10}A_{11}A_{00}$ is mapped (projects) in $\mathcal{B}_3$ to a closed walk running once along every loop, so that its *net voltage* (*i.e.* the sum of vector labels over the loops that are crossed along the walk in $\mathcal{B}_3$, which corresponds to the increments in the indices ij along the ring in **hxl**) is $10 + 01 + \overline{11} = 00$. Now the net voltage over the same closed walk in the quotient graph of **pcu** is 111. We deduce that **hxl** is isomorphic to the quotient of **pcu** by the subgroup generated by the translation 111, which may be written as **hxl** $\simeq$ **pcu**/$\langle 111 \rangle$. Formally, the quotient operation by a translation subgroup of **pcu** may be interpreted as the congruence relationship $111 \equiv 000$. In particular, this congruence leads to $001 \equiv \overline{110}$ so that we may first replace the voltage 001 by $\overline{110}$ in the labelled quotient graph of **pcu** and then drop the third useless zero index, common to every voltage of $\mathcal{B}_3$, to obtain the labelled quotient graph of **hxl**. Finally, we observe that the quotient relationship between the two nets is clearly associated with a projection relationship between their embeddings, which has been highlighted in Fig. 1. It happens that a maximum-symmetry embedding of **hxl** (*p*6*mm*, No. 17) in Euclidian space is obtained by orthogonal projection of a maximum-symmetry embedding of **pcu** ($Pm\overline{3}m$, No. 221) along the crystallographic direction [111].

2.2. Lattice and co-lattice vectors

Fig. 2 shows the 2-cycle $\mathcal{C}_2$ with voltage assignment in $\mathbb{Z}$ and three possible embeddings in $\mathbb{E}^2$ of the derived 1-periodic graph. Instead of defining the embedding by mapping the two edges e_1 and e_2 on two vectors in the plane, one may use the lattice vector **a** associated with the cycle $e_1 - e_2$ and the co-lattice vector L_A^* associated with the *co-boundary* $e_1 + e_2$ of vertex A in $\mathcal{C}_2$. (The co-boundary of some vertex is defined as the sum of incident edges with outgoing orientation at this vertex.) Because the mapping is linear by assumption, both descriptions are mathematically equivalent but the latter helps to clarify how the overall symmetry of the embedding depends on the local distortion at points A through the associated co-lattice vector L_A^*. To see this, call C the centre of gravity of the two B neighbours of a point A; it is readily seen that $L_A^* = 2\mathbf{AC}$. Hence the co-lattice vector at some point, being equal to the distance vector from this point to the centre of gravity of its neighbours multiplied by its degree, is a measure of the local distortion with respect to a barycentric embedding. Since distortions are opposed at points B (by definition $L_B^* = -e_1 - e_2$), the more general embedding drawn in Fig. 2(*a*) displays an inevitable two-fold rotation, in fact associated with the combinatorial symmetry $(e_1, \bar{e}_1)(e_2, \bar{e}_2)$ of $\mathcal{C}_2$. If L_A^* is orthogonal to the lattice vector **a**, a reflection symmetry is added to the embedding as seen in Fig. 2(*b*). This reflection corresponds to the combinatorial symmetry (e_1, e_2) of $\mathcal{C}_2$. The barycentric embedding shown in Fig. 2(*c*) corresponds to $L_A^* = 0$ and displays a new translation symmetry with lattice vector **a**/2, this time associated with combinatorial symmetry $(e_1, \bar{e}_2)$ of $\mathcal{C}_2$.

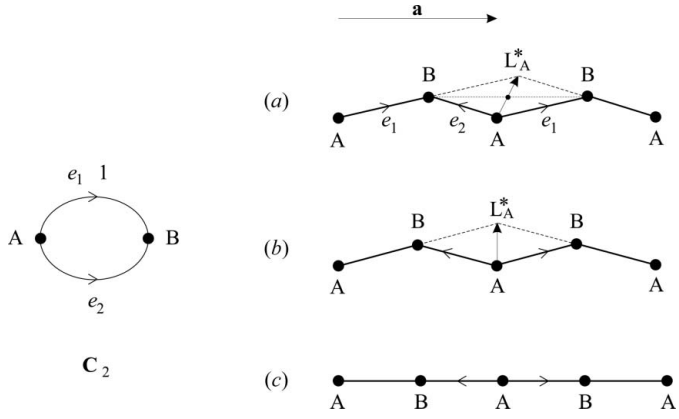

Figure 2
$\mathcal{C}_2$ with voltage assignment in $\mathbb{Z}$ and possible embeddings of the derived 1-periodic graph with (*a*) an arbitrary distortion L_A^*, (*b*) L_A^* orthogonal to lattice vectors, and (*c*) no distortion (barycentric embedding).

3. Quotient graphs and voltage graphs

Let $G = (V, E, i)$ be a graph, possibly containing loops and multiple edges (some authors speak then of a *multigraph* or *pseudograph*), defined on two disjoint sets, the vertex set $V = V(G)$ and the edge set $E = E(G)$, by the incidence mapping

$$i : e \longmapsto i(e) = \{u, v\}$$

for $e \in E$, $(u, v) \in V^2$ with $v = u$ if e is a loop; the incidence relation will be noted $e \sim \{u, v\}$. This definition of G as a triple is essential for handling graphs with loops and multiple edges.

For simplicity, members of the union set $X(G) = V(G) \cup E(G)$ are called *elements* of the graph. A graph automorphism φ is a permutation on $X(G)$, whose restrictions to $V(G)$ and $E(G)$ are permutations on these sets that are consistent with the incidence relationship, *i.e.* $\varphi(e) \sim \{\varphi(u), \varphi(v)\}$ for any edge $e \sim \{u, v\}$. Let $\mathrm{Aut}(G)$ denote the automorphism group of G. A non-trivial automorphism *acts freely* on the graph if it admits no fixed elements $x = \varphi(x)$ for $x \in X(G)$. Let $\mathcal{F}$ be a subgroup of $\mathrm{Aut}(G)$ which acts freely on G and denote by $[x]_{\mathcal{F}}$ the orbit of $x \in X(G)$ by $\mathcal{F}$ (*i.e.* the set of all the images of x by $\mathcal{F}$). The *regular quotient* $G/\mathcal{F}$ is the graph of the orbits defined as follows,

$$V(G/\mathcal{F}) = \{[u]_\mathcal{F} : u \in V\},$$

$$E(G/\mathcal{F}) = \{[e]_\mathcal{F} : e \in E\},$$

$$[e]_\mathcal{F} \sim \{[u]_\mathcal{F}, [v]_\mathcal{F}\} \text{ iff } e \sim \{x, y\} \text{ for some } x \in [u]_\mathcal{F}, y \in [v]_\mathcal{F}.$$

To define an *orientation* σ on a graph G, we introduce a digraph $G^\pm = (V, E^\pm, i^\pm)$ on the same vertex set V, where

(1) $\sigma : E^\pm \longrightarrow E$ is a two-to-one, onto mapping, so that we may arbitrarily note e^+ and e^-, the two arcs mapped on an edge e with

(2) $i^\pm(e^+) = (u, v)$ and $i^\pm(e^-) = (v, u)$ for $e \sim \{u, v\}$.

The incidence relation in $G^\pm$ will be noted $e^+ \sim uv$ and $e^- \sim vu$. We shall refer to G as the underlying graph to $G^\pm$. In practice, we simply indicate the positive arc, e^+, of $G^\pm$ by drawing an arrow on each edge e of G. It is worth noting that the definition also applies to graphs with multiple edges and an arbitrary number of loops on each vertex, which *per se* fully justifies the complexity of the construction.

An automorphism of a graph with an orientation is a permutation of both the vertex and arc sets, which is consistent with the incidence mapping and is invariant by reversal of the signs. We shall frequently represent an automorphism by its arc permutation using the cyclic notation since corresponding vertex permutations can easily be deduced. Instances of such automorphisms include loop inversions (e^+, e^-), or fourth-order permutations such as $(e_1^+, e_2^+, e_1^-, e_2^-)$ for two loops e_1 and e_2 at the same vertex. If G has no loops, then $\mathrm{Aut}(G^\pm) \simeq \mathrm{Aut}(G)$.

A *voltage assignment* in a group $\mathcal{A}$ on a graph G with an orientation σ is a mapping $\alpha : E^\pm \longrightarrow \mathcal{A}$ such that $\alpha(e^-) = [\alpha(e^+)]^{-1}$, where a^{-1} designates the inverse of a in $\mathcal{A}$. In the context of this contribution, voltages are vector labels from $\mathcal{A} = Z^p$ for generating p-periodic nets. Only voltages corresponding to the positive orientation of the edge are indicated on the graph, as for example in the two labelled quotient graphs of **hxl** and **pcu** in Fig. 1. Given a graph G with an orientation σ and voltage assignment α in a group $\mathcal{A}$, the *derived digraph* has vertex set $V \times \mathcal{A}$, arc set $E^\pm \times \mathcal{A}$ and incidence relation $(e, a) \sim (u, a)(v, ab)$ for $e \sim uv$ with $a, b = \alpha(e) \in \mathcal{A}$. The *derived graph* $D = G^\alpha$ is the underlying graph to the derived digraph (denoted by $D^\pm$). The group $\mathcal{A}$ acts freely on the derived graph if the action of $f \in \mathcal{A}$ on the element (vertex or edge) $(x, a) \in G^\alpha$ is given by $f[(x, a)] = (x, fa)$ (Gross & Tucker, 2001).

4. Periodic nets and their quotient graphs

Definition 4.1. A net is a simple 3-connected graph, which is locally finite (*i.e.* every vertex has finite degree).

Definition 4.2. A p-periodic net is a pair $(N, \mathcal{T})$ where N is a net and $\mathcal{T} \leq \mathrm{Aut}(N)$ is a free Abelian group of automorphisms of rank p, called the translation group of the net, such that the number of vertex and edge orbits by $\mathcal{T}$ in N is finite.

The above definition does not require that $\mathcal{T}$ be maximal in $\mathrm{Aut}(N)$. Indeed, periodic distortions may reduce the translational symmetry in some crystal structures. An example is α-cristobalite (low-temperature), whose topology is better described by that of diamond since, after substitution of Si—O—Si links by simple Si—Si links, the two structures are represented by isomorphic nets. However, the primitive unit cell of diamond contains two C atoms while that of α-cristobalite contains four Si atoms. In this case, the translational isometry group of α-cristobalite corresponds to a subgroup of index two of the combinatorial translation group of the associated net. Because we want to find an embedding of the net that describes the real crystal structure, we must consider the translational isometry subgroup $\mathcal{T}$ of the embedding at the expense of the full combinatorial translation group of the net in the definition of the periodic net $(N, \mathcal{T})$. Hence, although α-cristobalite and diamond are isomorphic as nets, they are not isomorphic as 3-periodic nets. Note that a careful analysis of the labelled quotient graph $N/\mathcal{T}$ still allows the full combinatorial translation group of the net N to be determined (Eon, 2005).

Proposition 4.1. The translation group $\mathcal{T}$ of a periodic net $(N, \mathcal{T})$ acts freely on the net N.

Proof. Suppose that some non-trivial translation $t \in \mathcal{T}$ fixes an edge $e \sim \{u, v\}$; clearly t^2 is a non-trivial translation fixing both vertices u and v. It is then sufficient to prove that no non-trivial translation can fix a vertex. Let $t \in \mathcal{T}$ be such a translation fixing a vertex u. Then, for any $\tau \in \mathcal{T}$, we have $t \cdot \tau(u) = \tau \cdot t(u) = \tau(u)$, so that t fixes the whole orbit $[u]_\mathcal{T}$ of u by $\mathcal{T}$. Take now a vertex v not in $[u]_\mathcal{T}$; its orbit $[v]_t$ by $\langle t \rangle$ (the free subgroup generated by t) is finite since every vertex in $[v]_t$ is at a fixed distance from u, and N is locally finite. We can thus find some non-trivial automorphism in $\langle t \rangle$ that fixes v, and hence fixes the whole orbit $[v]_\mathcal{T}$. Since the number of orbits in N is finite, the argument can be repeated until we find a non-trivial automorphism in $\langle t \rangle$ that fixes the whole vertex set of N, a contradiction in a free group. □

As especially important for its applications in solid state chemistry, we recall the following definition (Klee, 2004), based on the abstract definition of a space group (Schwarzenberger, 1980).

Definition 4.3. A crystallographic net is a periodic net whose automorphism group is isomorphic to an abstract space group.

By virtue of Proposition 4.1, the quotient graph $N/\mathcal{T}$ of a periodic net $(N, \mathcal{T})$ is a regular quotient. This property ensures that $N/\mathcal{T}$ describes faithfully the first neighbourhood of every vertex of the net (see Gross & Tucker, 2001). The quotient graph, however, fails to represent the overall topology of the net. Let us recall from Harary (1972) that the *cyclomatic number* c of a finite graph $G = (V, E, i)$ represents the number of independent cycles in G and is given by $c = |E| - |V| + 1$, where $|X|$ is the cardinality of the set X. From a graph with cyclomatic number $c > 1$ one can derive, up to isomorphism, infinitely many p-periodic graphs with $0 < p < c$. It is then necessary to use a voltage graph with voltage assignment in $\mathcal{T}$ to obtain, up to isomorphism, a one-

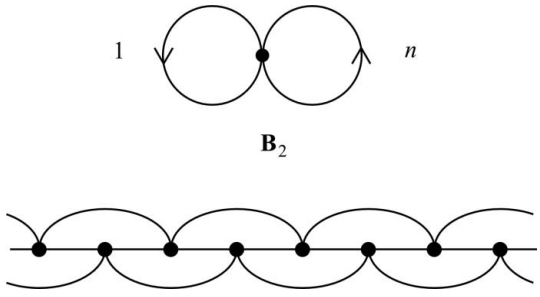

Figure 3
$\mathcal{B}_2$ with voltage assignment in $\mathbb{Z}$ and the 1-periodic net derived for $n = 2$.

to-one mapping between the periodic net and its labelled quotient graph (Chung *et al.*, 1984). Consider, for example, the bouquet $\mathcal{B}_2$ with voltage assignment in $\mathbb{Z}$ shown in Fig. 3. Any value of $n \geq 2$ yields a 1-periodic net with translation group isomorphic to $\mathbb{Z}$. The figure displays the 1-periodic net derived for $n = 2$. This net is but an example of a *lattice net*, as defined by Delgado-Friedrichs & O'Keeffe (2009).

In contrast, from a finite connected graph G of cyclomatic number $c > 0$, one can derive a unique c-periodic net, up to isomorphism: this net is called a *minimal net* (Beukemann & Klee, 1992) and denoted $M(G)$. Every periodic net derived from G can be described as a quotient of $M(G)$ by some translation subgroup.

5. Euclidian representations of periodic nets

Let G be a connected graph with an orientation σ containing n vertices and m edges, with a voltage assignment α in $\mathbb{Z}^p$. According to Godsil & Royle (2004), we define a *representation* of a net N in the Euclidian space $\mathbb{E}^r$ as a mapping

$$\rho : X(N) \rightarrow \mathbb{E}^r$$

such that every vertex u is mapped on a point $\rho(u)$ and every edge $e \sim \{u, v\}$ is mapped on the line segment $\rho(e) = \rho(u)\rho(v)$. A *periodic representation* of the derived net $N = G^\alpha$ is realized when vertices and edges of G are embedded, respectively, as point lattices and line lattices of rank p in $\mathbb{E}^r$. We call r the *dimension* of the representation. Note that the definition permits $p \leq r \leq m$; we shall speak of a *subperiodic* representation if $p < r$. Instead of the net N, one may advantageously consider the derived digraph $N^\pm$. In a periodic representation of $N^\pm$, every arc of $G^\pm$ is mapped on an *oriented line lattice*. Since any two arcs e^+ and e^-, pre-images for σ of some edge e in G, are incident to the same vertices, they will be embedded as the same line lattice. But as oriented line lattices, they have opposite orientation. This observation allows us to transcribe the incidence relationship in $G^\pm$: $e^+ \sim uv$ as an affine relation in the periodic representation of $N^\pm$:

$$\rho(v) = \rho(u) + \omega(e^+),$$

where ω maps the arc set of $G^\pm$ to $\mathbb{R}^r$, with the constraint $\omega(e^-) = -\omega(e^+)$. We may now determine a periodic representation of $N^\pm$ using the properties of the edge space of its quotient graph. Recall that the edge space is formally defined as the vector space admitting the edges of G as basis vectors. It is known that the edge space is the direct sum of the cycle and co-cycle spaces of the graph (Godsil & Royle, 2004).

Let $\mathbb{C}$ and $\mathbb{S}$ denote, respectively, the cycle and cut (or co-cycle) spaces of $G^\pm$, defined on the field of real numbers. As the basis of the cycle space, we shall take the m 2-cycles, $e^+ + e^-$, formed by all the pairs of opposite arcs (e^+, e^-) when e runs over the edge set of G, and complete the basis with a cycle basis of G, which we call $\mathcal{B}_c$, taking into account the orientation σ. We emphasize that $G^\pm$ is a directed graph, hence the cycles we consider here are directed cycles, *i.e.* combinations of arcs that are all forward. We recall that a *co-boundary* of a subset U of vertices is defined by Harary (1972) as the combination of edges joining the vertices of U to the vertices that are not in U. The co-cycle space is defined as the subspace of the edge space containing all the linear combinations of co-boundaries; this space is generated by the set of co-boundaries of single vertices. Taking into account the orientation of G, we may associate a co-cycle vector with every vertex by taking the sum of all the arcs of $G^\pm$ with outward orientation from this vertex. (Rigorously, one should use the sum of all incident arcs counting positively outward arcs and negatively inward arcs; the given choice yields the same result since the 2-cycles $(e^+ + e^-)$ are subsequently mapped to zero.) It is readily verified that the sum of these co-cycle vectors over the whole vertex set is exactly equal to the sum of the m 2-cycles $(e^+ + e^-)$. Hence, the co-cycle basis $\mathcal{B}_s$ should contain only a subset of $n - 1$ co-cycle vectors chosen among this set. For further convenience, we introduce the following definition.

Definition 5.1. A *co-lattice* in $\mathbb{R}^r$ is a set of n vectors L_i^* associated with the above-defined co-cycle vectors, with $\sum_i L_i^* = 0$.

Note that the rank of a co-lattice is arbitrary.

Proposition 5.1. A periodic representation in $\mathbb{E}^r$ of a p-periodic net derived from a finite graph G with voltage assignment in $\mathbb{Z}^p$ is uniquely determined, up to translation, by a lattice basis of rank p together with a co-lattice in $\mathbb{R}^r$.

Proof. Call B the $2m \times 2m$ matrix built as follows: the first m rows correspond to the 2-cycles formed by opposite arcs, the next $(m - n + 1)$ rows correspond to the vectors of the cycle basis $\mathcal{B}_c$, and the remaining $(n - 1)$ rows form a basis $\mathcal{B}_s$ of the co-cycle space $\mathbb{S}$ expressed in the standard basis of the edge-space of G, taking into account the orientation σ. We order the columns of B, writing first the positive arcs and then the negative arcs listed in the same sequence, yielding the following square block matrix,

$$\mathsf{B} = \begin{pmatrix} \mathsf{I}_m & \mathsf{I}_m \\ \mathsf{X} & \mathsf{Y} \end{pmatrix},$$

where I_m is the $m \times m$ unit matrix. The ij entry in matrix B gives the coefficient of edge e_j in the (cycle or co-cycle) basis vector i. Then, we define the $2m \times 1$ column vector

$$\Omega = \begin{pmatrix} \Omega^+ \\ \Omega^- \end{pmatrix},$$

in which the first m rows correspond to the vectors $\omega(e^+)$ and the last m rows to $\omega(e^-)$ when e runs over the edge set of G.

In a periodic representation of the derived net G^α in the Euclidian space $\mathbb{E}^r$ the cycle vectors of $G^\pm$ are mapped on translation vectors given by the net voltages over the corresponding closed walks. Let $\alpha(\mathsf{B})$ be an $m \times r$ matrix whose $(m - n + 1)$ first rows are the lattice vectors associated with net voltages over the basis vectors of $\mathcal{B}_c$ and the remaining rows correspond to a co-lattice in $\mathbb{R}^r$. The previous observations may be expressed in matrix form as follows,

$$\mathsf{B}\Omega = \begin{pmatrix} \Omega^+ + \Omega^- \\ \mathsf{X}\Omega^+ + \mathsf{Y}\Omega^- \end{pmatrix} = \begin{pmatrix} 0 \\ \alpha(\mathsf{B}) \end{pmatrix},$$

from which we derive

$$\begin{cases} \Omega^+ + \Omega^- &= 0 \\ \mathsf{X}\Omega^+ + \mathsf{Y}\Omega^- &= \alpha(\mathsf{B}) \end{cases} \quad \text{or} \quad \begin{cases} \Omega^- &= -\Omega^+ \\ \Omega^+ &= (\mathsf{X} - \mathsf{Y})^{-1}\alpha(\mathsf{B}). \end{cases}$$

Hence, $\alpha(\mathsf{B})$ uniquely determines, up to translation, a periodic representation of the derived net G^α mapping the positive arcs of $G^\pm$ on the rows of the matrix

$$\Omega^+ = (\mathsf{X} - \mathsf{Y})^{-1}\alpha(\mathsf{B}), \tag{1}$$

which we call the *arc matrix* for simplification. □

Observe that the entries of matrices X and Y are the coefficients (0 or 1) of positive and negative arcs, respectively, in the basis vectors of $\mathcal{B}_c$ and $\mathcal{B}_s$. Because an edge can only contribute as a positive or as a negative arc in a directed cycle or co-cycle, the entries of the difference matrix $(\mathsf{X} - \mathsf{Y})$ are $+1$ if the edge contributes as a positive arc, -1 if it contributes as a negative arc, and 0 if it does not contribute to the basis vector. As the change-of-basis matrix between two equivalent bases in the edge space, the edge basis and the cycle–co-cycle basis, the difference matrix $(\mathsf{X} - \mathsf{Y})$ is non-singular (Godsil & Royle, 2004).

We have seen above that opposite arcs e^+ and e^- are embedded as opposite lines in Euclidian space, $\omega(e^+)$ and $\omega(e^-)$. In the elaboration of the cycle–co-cycle matrix $\mathsf{X} - \mathsf{Y}$, the two arcs behave as though the respective edge vectors were opposite in the edge space. Needless to say, this was precisely the aim pursued with the definition of $G^\pm$. In the remainder of this paper we shall make this achievement explicit by setting that, as edge vectors, $e^- = -e^+$, where e runs over the edge set of G. This convention amounts to working in the quotient of the cycle space of $G^\pm$ by the subspace generated by the m 2-cycles $e^+ + e^-$ instead of working in the full cycle space. For short, we shall define the simplified cycle–co-cycle matrix $\mathsf{B}^* = \mathsf{X} - \mathsf{Y}$. We now consider a particularly important kind of representation.

Definition 5.2. We say that a representation of G^α is barycentric when all the vectors in the co-lattice are the null vector.

Barycentric representations of periodic nets have already been explored by Eon (1999) and Delgado-Friedrichs (2004, 2005). The fact that the sum of the outgoing arcs at every vertex is null justifies the epithet barycentric. There is also an interpretation in terms of the spectrum of the net. Consider the vector X^i $(i = 1, \ldots, p)$ in the vertex space of the net, whose component x^i_j is the ith coordinate of the point M_j representing vertex j (this index runs over the infinite set $\mathbb{Z}^p$). In a barycentric representation, these points satisfy the relation $\sum_{k\sim j} \overrightarrow{M_jM_k} = 0$ for every vertex j, where the sum is over the neighbours k of j. This yields for the ith coordinate $\sum_{k\sim j}(x^i_k - x^i_j) = \sum_{k\sim j} x^i_k - r_j x^i_j = 0$, where r_j is the degree of vertex j, and shows that X^i is an eigenvector of the Laplacian matrix of the net associated with the eigenvalue $\lambda = 0$ [see Godsil & Royle (2004) for more details about Laplacian matrices]. In fact, a related linear system is solved by *SYSTRE* to determine vertex coordinates of a net in an equilibrium placement.

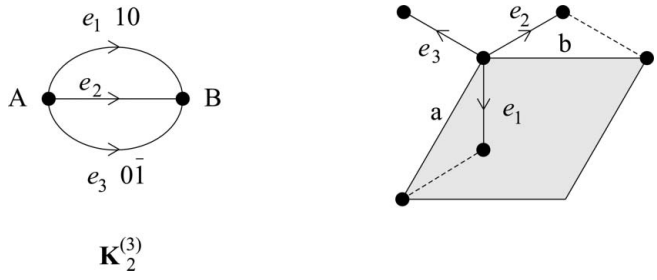

Figure 4
$\mathcal{K}_2^{(3)}$ with voltage assignment in $\mathbb{Z}^2$ and a 2-periodic representation of the derived net highlighting the unit cell.

Notice that Proposition 5.1 extends Theorem 4 of Delgado-Friedrichs (2005), which proved the uniqueness of the barycentric placement of a periodic net, given a lattice basis. The method described here provides a unique representation, whatever the image of the co-cycle basis vectors, *i.e.* it extends the embedding's existence and uniqueness results to non-barycentric representations. This means in particular that the geometry of any real crystal structure is completely determined, besides by its lattice basis, by its co-lattice. Each co-lattice vector L^*_i is equal to the distance vector from the respective atom M_i to the centre of gravity C of its first neighbours multiplied by its degree,

$$L^*_i = \sum_{k\sim i} M_iM_k = \sum_{k\sim i} M_iM_k + \sum_{k\sim i} M_kC = r_iM_iC.$$

5.1. The hexagonal net

As a simple example of a barycentric representation, let us consider the hexagonal net **hcb**; Fig. 4 displays its quotient graph $\mathcal{K}_2^{(3)}$ (the graph with two vertices and triple edges) with voltage assignment in $\mathbb{Z}^2$. The bases of the cycle and co-cycle space are given by

$$\mathcal{B}_c = \{e_1 - e_2, e_2 - e_3\}, \quad \mathcal{B}_s = \{e_1 + e_2 + e_3\},$$

from which we derive matrix $\mathsf{B}^* = \mathsf{X} - \mathsf{Y}$ and its inverse (the first row of B^* for instance reads $1 \times e_1 - 1 \times e_2 + 0 \times e_3 = e_1 - e_2$),

$$\mathsf{B}^* = \begin{pmatrix} 1 & -1 & 0 \\ 0 & 1 & -1 \\ 1 & 1 & 1 \end{pmatrix}, \quad \mathsf{B}^{*-1} = \begin{pmatrix} 2/3 & 1/3 & 1/3 \\ -1/3 & 1/3 & 1/3 \\ -1/3 & -2/3 & 1/3 \end{pmatrix}.$$

Reading the net voltages for each cycle on the graph $\mathcal{K}_2^{(3)}$ and adding the zero row for the co-lattice vector yields

$$\alpha(\mathsf{B}) = \begin{pmatrix} 1 & 0 \\ 0 & 1 \\ 0 & 0 \end{pmatrix}, \quad \Omega^+ = \mathsf{B}^{*-1}\alpha(\mathsf{B}) = \begin{pmatrix} 2/3 & 1/3 \\ -1/3 & 1/3 \\ -1/3 & -2/3 \end{pmatrix},$$

where the lattice basis (a, b) has been used as the basis of $\mathbb{E}^2$. The results are shown in the right-hand part of Fig. 4 where it can be seen that the derived net is the honeycomb, or hexagonal net, drawn here in its most symmetrical representation. The lattice vectors, however, are not determined by the above results and further analysis is necessary to find the Bravais lattice type; this analysis is postponed to §7.

6. Embeddings

Chemical properties impose severe restrictions to representations of periodic nets describing the topology of crystal structures. The question was thoroughly discussed by Delgado-Friedrichs *et al.* (2005), where it was suggested that, for generalized nets, the distance between non-linked points could be shorter than the distance between linked points, depending on the flexibility of the linkers. We shall thus conform to those authors and disregard distance considerations as long as they are not null. We say that a representation presents *crossings* when it is not injective, *i.e.* when two non-adjacent edges are represented as intersecting lines. According to the terminology in use in topological graph theory (Gross & Tucker, 2001), we shall use the following definition.

Definition 6.1. The image in Euclidian space of a periodic net by a periodic representation is called an *embedding* if this representation has no crossings.

Eventually, we shall say that an embedding is a *good embedding* if the distance between non-bonded points is strictly larger than the length of any line.

Notice that Delgado-Friedrichs & O'Keeffe (2005) call a *faithful embedding* what we simply refer to as an embedding. We prefer to specify it explicitly when a representation does present crossings. It may be useful also to distinguish the case where distinct vertices of the net have superposed images by the representation; we will then say that the representation presents *collisions*, which is clearly a special case of crossings. A net was said to be stable in Delgado-Friedrichs & O'Keeffe (2005) when its barycentric representation does not present collisions, which does not prevent the occurrence of crossings.

Definition 6.2. The *integral embedding* of a minimal net is defined as the image by the identity representation of $G^{\pm}$ in $\mathbb{E}^m$ with positive arcs given by $\Omega^+ = \mathsf{I}_m$, where I_m is the $m \times m$ unit matrix.

As a simple example, consider the 1-periodic graph derived from the 2-cycle $\mathcal{C}_2$ with edge labels given in Fig. 2. This graph is not a minimal net since it is not 3-connected but we may nonetheless define an integral embedding by representing its oriented edges e_1 and e_2 by two basis vectors $\mathbf{e}_1$ and $\mathbf{e}_2$ of $\mathbb{E}^2$. We may look at this embedding as an infinite flight of stairs in the direction $1\bar{1}$.

It was shown by Eon (1999) that the above representation provides indeed an embedding for any minimal net in $\mathbb{E}^m$. Since the periodicity of minimal nets is equal to the cyclomatic number of their quotient graph $c(G) = m - n + 1 \leq m$, the integral embedding is generally subperiodic, with finite extension along the co-cycle space. Integral embeddings are thus generalizations of layer structures.

6.1. The minimal net derived from the dumbbell graph

Fig. 5 shows the dumbbell graph, a graph with two loops and a *bridge* (a cut edge), with voltage assignment in $\mathbb{Z}^2$ and a 2-periodic representation of the derived (minimal) net. Since a bridge belongs to the co-cycle space of the graph, the corresponding line lattice must collapse in any barycentric representation of the net. Any non-barycentric representation in $\mathbb{E}^2$ displays a crossing of the two line lattices mapped by the loops. The 2-periodic integral embedding in $\mathbb{E}^3$ avoids crossings but displays non-bonded points at the same distance as bonded points, hence there is no good embedding of the net derived from the dumbbell graph. Note that a good embedding of the net in $\mathbb{E}^3$ has been exhibited by Koch & Fischer (1978), as the non-planar sphere packing *KIa*, but the unit cell needs to be duplicated in both crystallographic directions, as drawn in Fig. 6. The quotient graph of the net by the corresponding subgroup of index 4 has thus $4 \times 2 = 8$ vertices and $4 \times 3 = 12$ edges, hence cyclomatic number $c = 5$, as shown in Fig. 6. In accordance with Definition 4.2, *KIa* as a periodic net is not isomorphic to the minimal net derived from the dumbbell graph.

7. Symmetry and metric tensor

We first focus on crystallographic nets and some special embeddings. Algebraic methods are used to determine the

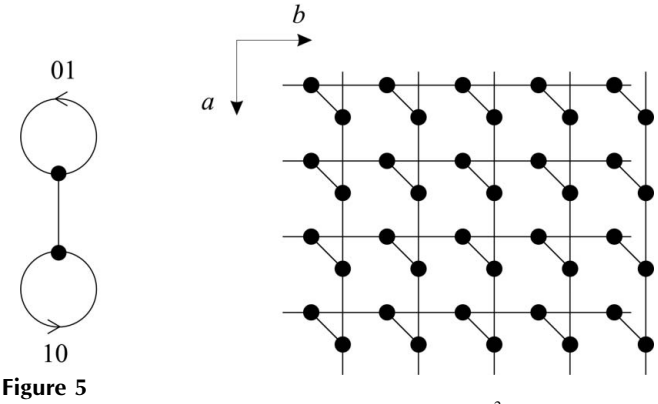

Figure 5
A graph with a bridge and voltage assignment in $\mathbb{Z}^2$, and a 2-periodic representation of the derived net.

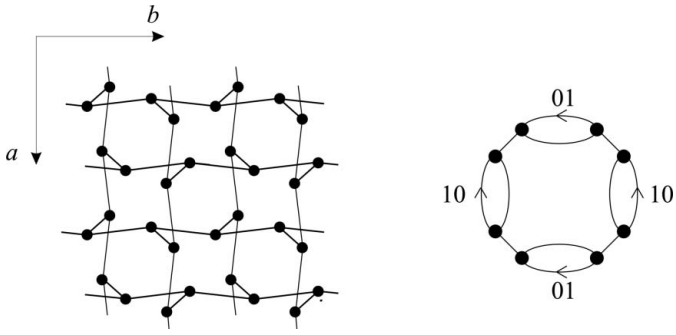

Figure 6
A 2-periodic embedding in $\mathbb{E}^3$ of the minimal net derived from the dumbbell graph and its *expanded* quotient graph with voltage assignment in $\mathbb{Z}^2$.

space-group type of the net from the structure of the labelled quotient graph. They require the analysis of usual invariants, such as determinant and trace of a linear representation of the point-group operations and their order. The technique will be illustrated in the case of α-cristobalite in §9; more details may be found in Eon (1998) and Klee (2004). In this section we formulate the main relations between the different symmetry groups in presence.

Theorem 7.1. Let $(N, \mathcal{T})$ be a crystallographic net of quotient graph $G = N/\mathcal{T}$ with voltage assignments in $\mathcal{T}$; the factor group $\mathrm{Aut}(N)/\mathcal{T}$ is isomorphic to the subgroup $H(\mathcal{K})$ of $\mathrm{Aut}(G^{\pm})$ that stabilizes the subspace $\mathcal{K}$ of cycle vectors of G with zero net voltage.

Proof. Because a net N is a simple graph, we have $\mathrm{Aut}(N^{\pm}) \simeq \mathrm{Aut}(N)$. It is thus equivalent to work on the net N or on the digraph $N^{\pm}$ derived from $G^{\pm}$. Since $\mathcal{T}$ is a normal subgroup of $\mathrm{Aut}(N)$, any automorphism φ_N of N induces an automorphism φ_G in $G^{\pm}$, defined by $\varphi_G([x]_T) = [\varphi_N(x)]_T$, where x is any vertex or edge of N. Now closed walks in the net project on cycle vectors of $G^{\pm}$ with zero net voltage and, conversely, cycle vectors of $G^{\pm}$ with zero net voltage are lifted to closed walks in the net. On the other hand, closed walks in the net are mapped on closed walks by φ_N, hence φ_G stabilizes the subspace $\mathcal{K}$. Because translations in $\mathcal{T}$ induce the identity of $\mathrm{Aut}(G^{\pm})$, two automorphisms of N in the same coset $\varphi_N\mathcal{T}$ induce the same automorphism of $G^{\pm}$. Conversely, any automorphism $\varphi_G \in H(\mathcal{K})$ induces, up to translation, a unique automorphism φ_N of the net, which may be defined as follows. We first set a vertex a as origin of the net and choose its image $\varphi_N(a)$ in the vertex lattice $\varphi_G([a]_T)$. To any vertex x of the net, we associate an arbitrary walk ax from a to x. Let w be the projection of this walk on $G^{\pm}$; then $\varphi_N(x)$ is defined as the end of the unique walk lifted from $\varphi_G(w)$ and starting at $\varphi_N(a)$. We will now show that φ_N is well defined and is indeed an automorphism of N.

Consider first a different walk between a and x which projects on a walk $w' \neq w$ in $G^{\pm}$. After reversing the orientation on w, we can form the cycle vector $w' - w \in \mathcal{K}$ (because it is the projection of a closed walk in N). By assumption, $\varphi_G(w') - \varphi_G(w) = \varphi_G(w' - w) \in \mathcal{K}$. Hence, the two walks $\varphi_G(w')$ and $\varphi_G(w)$ have the same starting vertex $\varphi_G([a]_T)$, the same end vertex $\varphi_G([x]_T)$ and the same net voltage, and so the walks lifted from them and starting at $\varphi_N(a)$ will end at the same vertex of N. The mapping sending $\varphi_N(a)$ back to a and lifted from φ_G^{-1} in the same way is clearly an inverse to φ_N, showing that this mapping realizes a permutation on the vertex set of N. Consider now two linked vertices $x \sim y$ in N and form a closed walk $axya$ running along the edge xy. Its projection w in $G^{\pm}$ is a closed walk of $\mathcal{K}$ running along $[x]_T[y]_T$, hence $\varphi_G(w) \in \mathcal{K}$ and runs along the edge $\varphi_G([x]_T)\varphi_G([y]_T)$. Lifting this closed walk from $\varphi_N(a)$, we find that $\varphi_N(x) \sim \varphi_N(y)$, showing that φ_N is an automorphism of N. We have then put into evidence a bijection between $\mathrm{Aut}(N)/\mathcal{T}$ and $H(\mathcal{K})$, which is readily verified to be a group isomorphism. □

We next observe that the space group of any embedding of the net is isomorphic to a subgroup of its automorphism group $\mathrm{Aut}(N)$. We shall rely on projection techniques to display a representation of a crystallographic net $(N, \mathcal{T})$ whose space group is isomorphic to $\mathrm{Aut}(N)$ provided it is an embedding of N. Firstly, we note that the standard basis of the co-cycle space of $G^{\pm}$ was interpreted as a set of displacements of each point from its barycentric position, hence it must be compatible with the operations of the symmetry group of the representation. This condition is trivially fulfilled in barycentric representations.

We now embed the net in the edge space of $G^{\pm}$, assuming that the natural basis $\{e_i \equiv e_i^+\}$ is orthonormal. As above, let $\mathcal{K}$ be the subspace of cycle vectors with zero net voltage in $G^{\pm}$. Call $\mathcal{P}$ the orthogonal projection in the edge space that admits $\mathcal{K}$ as its kernel; $\mathcal{P}$ enables the construction of a lattice in the edge space as follows. If $A = \sum_i \lambda_i e_i$ ($\lambda_i \in \mathbb{Z}$) is a cycle vector of $G^{\pm}$ with net voltage $\mathbf{a}$, we define the corresponding lattice vector by the projection $\mathcal{P}(A) = \sum_i \lambda_i \mathcal{P} e_i$. It is immediate that the definition is consistent: if $\mathcal{P}(A) = 0$, then $A \in \mathcal{K}$ and so $\mathbf{a} = \alpha(A) = 0$. As a consequence, if $\{A_i\}$ is a set of cycle vectors whose voltages $\{\mathbf{a}_i\}$ form a basis of the translation group $\mathcal{T}$, then $\{\mathcal{P}(A_i)\}$ forms the basis of a lattice $\mathcal{L}$ with the same rank. Since every cycle vector has net voltage in $\mathcal{T}$, it must project in $\mathcal{L}$.

The barycentric representation of the net built upon the lattice $\mathcal{L}$ will be called *archetypical*. Representations of minimal nets obtained in this way are called *archetypes* (in this case, $\mathcal{P}$ is the identity), so that archetypical representations are just orthogonal projections of the archetype. Note that archetypical representations realize the net as a quotient of the associated minimal net. Fig. 1, for instance, shows the archetypical representation of the net **hxl** as an orthogonal projection of the archetype associated with the minimal net **pcu** (in this case the archetype is an integral embedding). Several examples of archetypical representations of 2- and 3-periodic nets derived from the graph $\mathcal{K}_3^{(2)}$ will be constructed in §8.

Theorem 7.2. Let $(N, \mathcal{T})$ be a crystallographic net with archetypical embedding $\mathcal{E}$, then the space group $\Gamma(\mathcal{E})$ is isomorphic to $\mathrm{Aut}(N)$.

Proof. It is sufficient to prove that every automorphism in $H(\mathcal{K})$ induces an isometry in Euclidian space, which is a symmetry operation of $\Gamma(\mathcal{E})$. An automorphism $\varphi_G \in H(\mathcal{K})$, acting as a permutation on the arcs of $G^{\pm}$, induces a linear operator, say φ, in the edge space of $G^{\pm}$. It is readily verified that φ preserves the inner product in the edge space. Moreover, φ and $\mathcal{P}$ commute. To see this, let us analyze the properties of $\mathcal{Q} = \varphi^{-1}\mathcal{P}\varphi$:

(1) By hypothesis, φ stabilizes $\mathcal{K}$: $\varphi(\mathcal{K}) = \mathcal{K}$ and $\mathcal{P}(\mathcal{K}) = 0$, hence $\mathcal{Q}(\mathcal{K}) = 0$.

(2) Let $x \in \mathcal{K}^{\perp}$, then $\langle \varphi(x), \varphi(\mathcal{K})\rangle = \langle x, \mathcal{K}\rangle = 0$, where the brackets $\langle x, y\rangle$ denote the inner product of vectors x and y. Hence $\varphi(x) \in \mathcal{K}^{\perp}$ implying that $\mathcal{P}\varphi(x) = \varphi(x)$ and thus $\mathcal{Q}(x) = x$.

These two observations show that $\mathcal{Q}$ is a projection on $\mathcal{K}^{\perp}$ with kernel $\mathcal{K}$, so that $\mathcal{Q} = \mathcal{P}$. On the other hand, φ_G induces, through net voltages over cycles of $G^{\pm}$, a linear operator, say φ_T. The action on the lattice vector $\mathbf{a}$ derived from a cycle vector A is defined by $\varphi_T(\mathbf{a}) = \varphi_T\mathcal{P}(A) = \mathcal{P}\varphi(A)$, so that $\varphi_T\mathcal{P}(A) = \varphi\mathcal{P}(A)$. We first check that φ_T is well defined. If A' is another cycle vector of $G^{\pm}$ with the same net voltage $\mathbf{a}$, then $A' - A$ is a cycle vector with zero net voltage and so belongs to the subspace $\mathcal{K}$. Hence, $\mathcal{P}(A' - A) = 0$ and $\varphi\mathcal{P}(A') = \varphi\mathcal{P}(A)$, as desired. Suppose now that $\varphi\mathcal{P}(A) = \mathcal{P}\varphi(A) = \mathcal{P}(A)$; then $\varphi(A) - A \in \mathcal{K}$ so that $\varphi(A)$ has the same voltage as A. This shows that φ_T is trivial whenever φ_G is an automorphism that fixes every voltage in $G^{\pm}$. We know that such an automorphism is associated with a combinatorial translation symmetry in a crystallographic net (Eon, 2005). If $\mathcal{T}$ is a maximal translation group in Aut(N), then φ_G is the identical automorphism in $G^{\pm}$, from which we may conclude that φ_T is trivial if and only if φ_G is the identity.

We are now in a position to show the invariance by φ_T of the inner product between two lattice vectors $\mathbf{a}$ and $\mathbf{b}$ of $\mathcal{T}$ derived from the cycle vectors A and B of $G^{\pm}$:

$$\begin{aligned}\langle \varphi_T(\mathbf{a}), \varphi_T(\mathbf{b})\rangle &\equiv \langle \varphi_T\mathcal{P}(A), \varphi_T\mathcal{P}(B)\rangle \\ &= \langle \varphi\mathcal{P}(A), \varphi\mathcal{P}(B)\rangle \\ &= \langle \mathcal{P}(A), \mathcal{P}(B)\rangle \\ &= \langle \mathbf{a}, \mathbf{b}\rangle.\end{aligned}$$

By linearity of construction of the embedding, it follows that φ_T also permutes the line lattices of $\mathcal{E}$ and, consequently, it is the linear part of some isometry which maps $\Gamma(\mathcal{E})$ on itself. □

If L denotes the $p \times m$ matrix whose rows are cycle-vectors of $G^{\pm}$, expressed in the natural basis of the edge-space, which form a lattice basis of the p-periodic net, the metric tensor of the lattice is given by

$$\mathsf{Z} = \mathsf{L}\mathsf{P}\mathsf{L}^{t}.$$

Of course, the theorems concerning the existence, uniqueness and space-group type of barycentric embeddings for stable crystallographic nets were already known after the work of Delgado-Friedrichs & O'Keeffe (2003, 2005). The main advantage of the projection method exposed here is to effectively display such an embedding with the right symmetry and to provide its metric tensor in a very simple way.

7.1. Metric tensor of hcb

For minimal nets, the kernel $\mathcal{K}$ is reduced to {0} so that P is the unit matrix. In the case of the hexagonal net studied in §5.1, we obtain

$$\mathsf{L} = \begin{pmatrix} 1 & -1 & 0 \\ 0 & 1 & -1 \end{pmatrix}, \quad \mathsf{Z} = \begin{pmatrix} 2 & -1 \\ -1 & 2 \end{pmatrix}.$$

This metric tensor characterizes a hexagonal lattice (**a**, **b**) with $\mathbf{a}^2 = \mathbf{b}^2 = 2$ and $\angle(\mathbf{a}, \mathbf{b}) = 120^{\circ}$, as already pictured in Fig. 4. The space-group type of the embedding is *p*6*mm* and its crystallographic point group is 6*mm*, isomorphic to the automorphism group of $\mathcal{K}_2^{(3)}$ generated by the permutations (e_1, e_2), (e_1, e_3) and $(e_1, \overline{e}_1)(e_2, \overline{e}_2)(e_3, \overline{e}_3)$.

It is usually preferable to define directly φ_T by a transformation matrix in a lattice basis, which is easily performed using the net voltage over corresponding cycle vectors in the labelled quotient graph. A cycle vector C corresponds in the embedding to a lattice vector $L = \alpha(C)$, the net voltage over C. It is sent by φ_T to the lattice vector $\varphi_T(L) = \alpha[\varphi(C)]$. The essential meaning of Theorem 7.2 is that φ_T is an isometry of the lattice if this lattice belongs to the same Bravais lattice type as that determined by projection. But, instead of using the projection method, we may apply equation (1) to derive the embedding, be it barycentric or not. Let us denote by L_V^* the co-lattice vector mapped by the co-cycle basis vector at vertex V. Co-lattice vectors should transform according to point-group operations of the embedding,

$$\varphi_T(L_V^*) = L_{\varphi(V)}^*. \tag{2}$$

Corollary 7.1. Let L be a lattice in $\mathbb{R}^p$ belonging to the same Bravais lattice type as the archetypical lattice $\mathcal{L}$ and let L^* be a set of co-lattice vectors that transform according to the linear mapping φ_T as defined above. Then φ_T is a symmetry operation of the embedding derived from (L, L^*) by equation (1).

Proof. Consider a cycle or co-cycle basis vector C defined in the edge basis by $C = \sum \lambda_i e_i$. After embedding the net, this yields $\Lambda = \sum \lambda_i \omega(e_i)$, where Λ is the lattice or co-lattice vector associated with C. Hence, on applying φ_T, we find $\varphi_T(\Lambda) = \sum \lambda_i \varphi_T[\omega(e_i)]$. On the other hand, on applying the automorphism φ to the definition of C, we find $\varphi(C) = \sum \lambda_i \varphi(e_i)$. If C is a cycle vector associated with the lattice vector $\Lambda = \alpha(C)$, $\varphi(C)$ is embedded as the lattice vector $\alpha[\varphi(C)] = \varphi_T(\Lambda)$. If C is a co-cycle vector associated with the co-lattice vector $\Lambda = L_V^*$, $\varphi(C)$ is the co-cycle vector at $\varphi(V)$ and is embedded as the co-lattice vector $L_{\varphi(V)}^* = \varphi_T(\Lambda)$. In both cases, we find after embedding $\varphi_T(\Lambda) = \sum \lambda_i \omega[\varphi(e_i)]$. Comparing both results, we have

$$\forall \Lambda \in L \cup L^* \quad \varphi_T(\Lambda) = \sum \lambda_i \varphi_T[\omega(e_i)] = \sum \lambda_i \omega[\varphi(e_i)].$$

Since the coefficients λ_i are the entries of the non-singular cycle–co-cycle matrix, we find on inversion, for every edge e_i,

$$\varphi_T[\omega(e_i)] = \omega[\varphi(e_i)].$$

By construction, φ_T maps the embedding on itself; being also an isometry, φ_T is a symmetry operation of the embedding. □

7.2. Embeddings of lower symmetry of hcb

Corollary 7.1 provides a simple interpretation of the results exposed by Thimm (2009). As an example, consider the hexagonal net embedded with a hexagonal lattice. Since the net possesses two vertices per unit cell, the co-lattice vectors in the most general embedding are linearly dependent: $L_A^* + L_B^* = 0$ (see Definition 5.1). As a consequence, an arbitrary co-lattice is invariant by the inversion of the three edges, which is associated with the twofold rotation of the embedding. This symmetry operation is thus inevitable. Choosing the co-lattice vectors along 10, $1\bar{1}$ or an equivalent direction associated with a reflection plane will add this operation to the space group of the embedding. The threefold rotation will be allowed if the co-lattice vector is along the rotation axis, which imposes that it is the zero vector. In other words, only the barycentric embedding may have the full symmetry of the net.

8. Nets derived from $\mathcal{K}_3^{(2)}$

This section illustrates the application of the projection method to the determination of barycentric embeddings of stable crystallographic nets. We shall consider several 2-, 3- and 4-periodic nets derived from the graph $\mathcal{K}_3^{(2)}$, the graph of the triangle with double edges and cyclomatic number 4. It should be stressed that the list is not exhaustive. Other periodic nets, known and unknown, do admit this same graph as their quotient graph and can be studied by the projection method. Since the derived 2- and 3-periodic nets are nontrivial quotient nets of the 4-periodic minimal net, we need new algebraic tools to determine the projection matrix.

Let K be a matrix whose rows correspond to linearly independent vectors defining the kernel of some orthogonal projection in an orthonormal basis. Denote $\mathsf{S} = \mathsf{K} \cdot \mathsf{K}^t$ and I the unit matrix; it can be shown (Godsil & Royle, 2004) that the matrix of the projection is given by

$$\mathsf{P} = \mathsf{I} - \mathsf{K}^t \cdot \mathsf{S}^{-1} \cdot \mathsf{K}.$$

8.1. The hyperquartz net

The net **qtz** describes the simplified topology of quartz, where every Si—O—Si link is represented by a single edge. This net admits the graph $\mathcal{K}_3^{(2)}$ as its quotient graph, with voltage assignment shown in Fig. 7. Since the quotient has cyclomatic number 4, **qtz** is a quotient of the respective 4-periodic minimal net, which we call the *hyperquartz* net (Eon, 1998; Klee, 2004). The quotient graph of this net is given in Fig. 8(*a*) with voltage assignment in $\mathbb{Z}^4$. (Since it is a minimal net, this assignment is quite arbitrary. The two edges AB and AC were chosen as a spanning tree, each receiving zero voltage. Then simple, independent voltages 1000, 0100, *etc.* were attributed to each cycle defining a region in the plane.)

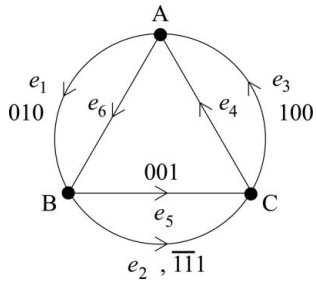

Figure 7
The labelled quotient graph of the quartz net.

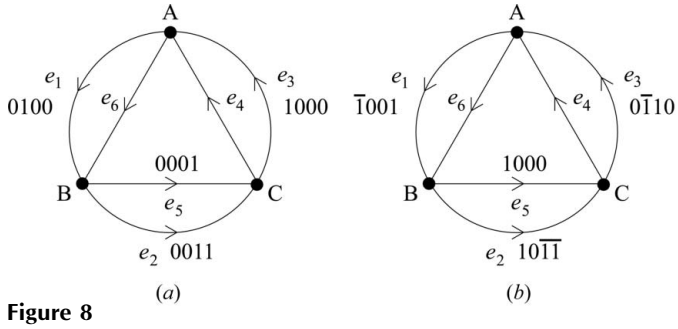

Figure 8
(*a*) The labelled quotient graph of the hyperquartz net. (*b*) Voltage assignment with a primitive basis in accordance with $\mathbb{Z}$-class 25/11/03 (Brown *et al.*, 1978).

As in the case of **hcb**, the kernel $\mathcal{K}$ is reduced to the co-cycle space of $\mathcal{K}_3^{(2)}$ so that we may use the unit matrix as projection matrix P to determine directly the metric tensor of hyperquartz. Extracting the expression of the lattice vectors from the quotient graph (the first row of L, for example, reads $1000 = 1 \times e_3 - 1 \times e_4$), we obtain

$$\mathsf{L} = \begin{pmatrix} 0 & 0 & 1 & -1 & 0 & 0 \\ 1 & 0 & 0 & 0 & 0 & -1 \\ 0 & 1 & 0 & 0 & -1 & 0 \\ 0 & 0 & 0 & 1 & 1 & 1 \end{pmatrix},$$

$$\mathsf{Z} = \begin{pmatrix} 2 & 0 & 0 & -1 \\ 0 & 2 & 0 & -1 \\ 0 & 0 & 2 & -1 \\ -1 & -1 & -1 & 3 \end{pmatrix}.$$

If we call (**a**, **b**, **c**, **d**) this lattice basis, we see that we can choose the new basis (**a**, **b**, **c**, **e** = **a** + **b** + **c** + 2**d**), which belongs to the cubic orthogonal family. Hence the unit cell is $\mathbb{Z}$-centred. The space-group type in the classification of four-dimensional crystallographic groups by Brown *et al.* (1978) was determined by Eon (1998) as 25/08/03/003. For reference, Fig. 8(*b*) shows a voltage assignment of $\mathcal{K}_3^{(2)}$ yielding the characteristic Bravais type XVII/IV metric tensor,

$$\mathbb{Z} = \begin{pmatrix} 3 & 0 & -1 & 2 \\ 0 & 3 & 2 & -1 \\ -1 & 2 & 3 & -2 \\ 2 & -1 & -2 & 3 \end{pmatrix}.$$

To obtain the fractional coordinates associated with this embedding, we invert the cycle–co-cycle matrix B^* and define the *voltage* matrix $\alpha(\mathsf{B})$ from the labelled quotient graph. Note that the $\mathbb{Z}$-centred cell (**a**, **b**, **c**, **e**) has been used here. The first row of B^*, for example, corresponds to the cycle $1 \times e_1 - 1 \times e_6$ whose net voltage, 0100, is given as the first row of $\alpha(\mathsf{B})$. The fourth row of B^* is the cycle vector $\sum_i e_1$ associated with the new lattice vector **e** with voltage 0001. The last two rows of B^* define the co-lattice, a basis of the co-cycle space, which is projected to zero and corresponds to the co-cycles formed at vertices A $(1 \times e_1 - 1 \times e_3 - 1 \times e_4 + 1 \times e_6)$ and B $(-1 \times e_1 + 1 \times e_2 + 1 \times e_5 - 1 \times e_6)$,

$$\mathsf{B}^* = \begin{pmatrix} 1 & 0 & 0 & 0 & 0 & \overline{1} \\ 0 & 1 & 0 & 0 & \overline{1} & 0 \\ 0 & 0 & 1 & \overline{1} & 0 & 0 \\ 1 & 1 & 1 & 1 & 1 & 1 \\ 1 & 0 & \overline{1} & \overline{1} & 0 & 1 \\ \overline{1} & 1 & 0 & 0 & 1 & \overline{1} \end{pmatrix}, \quad \alpha(\mathsf{B}) = \begin{pmatrix} 0 & 1 & 0 & 0 \\ 0 & 0 & 1 & 0 \\ 1 & 0 & 0 & 0 \\ 0 & 0 & 0 & 1 \\ 0 & 0 & 0 & 0 \\ 0 & 0 & 0 & 0 \end{pmatrix},$$

$$\Omega^+ = \mathsf{B}^{*-1} \cdot \alpha(\mathsf{B}) = \begin{pmatrix} 0 & 1/2 & 0 & 1/6 \\ 0 & 0 & 1/2 & 1/6 \\ 1/2 & 0 & 0 & 1/6 \\ -1/2 & 0 & 0 & 1/6 \\ 0 & 0 & -1/2 & 1/6 \\ 0 & -1/2 & 0 & 1/6 \end{pmatrix}.$$

If we set the first point at the origin, we obtain the following coordinates, given for the cubic orthogonal cell,

$$\begin{cases} A: & 0, 0, 0, 0 & (1/2, 1/2, 1/2, 1/2), \\ B: & 0, 1/2, 0, 1/6 & (1/2, 0, 1/2, 2/3), \\ C: & 0, 1/2, 1/2, 1/3 & (1/2, 0, 0, 5/6). \end{cases}$$

8.2. The quartz net

We will build a three-dimensional embedding of **qtz** as a projection of the respective four-dimensional archetype. The crystallographic direction of the projection is given by the closed trail $w = e_1 e_2 e_3 \overline{e}_4 \overline{e}_5 \overline{e}_6$, the shortest non-trivial closed walk of the quotient graph with zero net voltage. As a general rule to find the generators of the kernel of the projection, in the case of a 3-periodic net, one may choose three cycles of the quotient with independent net voltages. The net voltage of the remaining cycles in a cycle basis of the quotient graph may then be written as a combination of these voltages, thus providing as many cycle vectors with zero net voltage. For **qtz**, we choose $\alpha = e_3 - e_4$, $\beta = e_1 - e_6$ and $\gamma = e_4 + e_6 + e_5$ as basis cycles (regions of the plane) with independent net voltages 100, 010 and 001, respectively. The net voltage of the fourth independent 2-cycle $\delta = e_2 - e_5$ is then read as $\overline{1}10$, showing that the combination $\alpha + \beta + \delta = e_1 + e_2 + e_3 - e_4 - e_5 - e_6$ is a cycle vector with zero net voltage.

The following matrix K describes a basis for the kernel of the projection, taking into account both the cycle and co-cycle space. (The first row defines the above closed trail while the other two rows define the basis of the co-cycle space, providing for a barycentic representation.) By application of the above formula, we obtain then the projection matrix P,

$$\mathsf{K} = \begin{pmatrix} 1 & 1 & 1 & \overline{1} & \overline{1} & \overline{1} \\ 1 & 0 & \overline{1} & \overline{1} & 0 & 1 \\ \overline{1} & 1 & 0 & 0 & 1 & \overline{1} \end{pmatrix},$$

$$\mathsf{P} = \begin{pmatrix} 1/2 & 0 & 0 & 1/3 & 1/3 & -1/6 \\ 0 & 1/2 & 0 & 1/3 & -1/6 & 1/3 \\ 0 & 0 & 1/2 & -1/6 & 1/3 & 1/3 \\ 1/3 & 1/3 & -1/6 & 1/2 & 0 & 0 \\ 1/3 & -1/6 & 1/3 & 0 & 1/2 & 0 \\ -1/6 & 1/3 & 1/3 & 0 & 0 & 1/2 \end{pmatrix}.$$

We now write the matrix L whose rows provide the three cycles used as basis of the net **qtz**, expressed in the natural basis. (The first row, for example, reads $e_3 + \overline{e}_4$, the cycle with net voltage 100.) The matrix Z of the metric tensor can then be calculated,

$$\mathsf{L} = \begin{pmatrix} 0 & 0 & 1 & \overline{1} & 0 & 0 \\ 1 & 0 & 0 & 0 & 0 & \overline{1} \\ 0 & 0 & 0 & 1 & 1 & 1 \end{pmatrix},$$

$$\mathsf{Z} = \begin{pmatrix} 4/3 & -2/3 & 0 \\ -2/3 & 4/3 & 0 \\ 0 & 0 & 3/2 \end{pmatrix}.$$

The latter matrix is in agreement with Bravais type *hP*, with the ratio $c/a = 3\sqrt{2}/4 \simeq 1.061$, not far from the experimental value $c/a = 5.47/5.01 \simeq 1.092$.

To find the fractional coordinates associated with this embedding, we invert the cycle–co-cycle matrix B^* and define the *voltage* matrix $\alpha(\mathsf{B})$ from the labelled quotient graph [the first row of B, for example, corresponds to the cycle $e_1 + \overline{e}_6$ whose net voltage, 010, is given as the first row of $\alpha(\mathsf{B})$; the last two rows of B^* define a basis of the co-cycle space, which are projected to zero],

$$\mathsf{B}^* = \begin{pmatrix} 1 & 0 & 0 & 0 & 0 & \overline{1} \\ 0 & 1 & 0 & 0 & \overline{1} & 0 \\ 0 & 0 & 1 & \overline{1} & 0 & 0 \\ 0 & 0 & 0 & 1 & 1 & 1 \\ 1 & 0 & \overline{1} & \overline{1} & 0 & 1 \\ \overline{1} & 1 & 0 & 0 & 1 & \overline{1} \end{pmatrix}, \quad \alpha(\mathsf{B}) = \begin{pmatrix} 0 & 1 & 0 \\ \overline{1} & \overline{1} & 0 \\ 1 & 0 & 0 \\ 0 & 0 & 1 \\ 0 & 0 & 0 \\ 0 & 0 & 0 \end{pmatrix},$$

$$\Omega^+ = \mathsf{B}^{*-1} \cdot \alpha(\mathsf{B}) = \begin{pmatrix} 0 & 1/2 & 1/3 \\ -1/2 & -1/2 & 1/3 \\ 1/2 & 0 & 1/3 \\ -1/2 & 0 & 1/3 \\ 1/2 & 1/2 & 1/3 \\ 0 & -1/2 & 1/3 \end{pmatrix}.$$

Let us put point A at position $(1/2, 1/2, 2/3)$; the position of the remaining points is obtained from affine conditions, directly from the quotient graph [for example, $B = A + \omega(e_1)$].

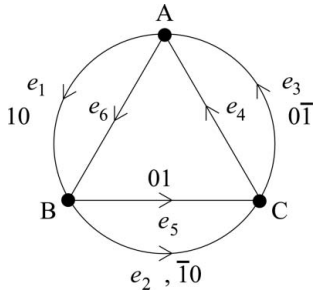

Figure 9
The labelled quotient graph of the Kagome net.

We obtain the following coordinates, corresponding to Wyckoff position 3*c*,

$$\begin{cases} A: & 1/2, & 1/2, & 2/3, \\ B: & 1/2, & 0, & 0, \\ C: & 0, & 1/2, & 1/3. \end{cases}$$

It may be verified that the space-group type of this embedding is $P6_422$ (No. 181); if, however, the sign of the component along the *c* axis is reversed for both voltages over e_2 and e_5, the enantiomorphic embedding with space-group type $P6_222$ is obtained. Of course, in this case, as in that of the next two-dimensional nets, the results are the same as given by *SYSTRE*.

8.3. The Kagome net

kgm is a two-dimensional net also admitting $\mathcal{K}_3^{(2)}$ as its quotient graph, as given in Fig. 9.

An embedding of this net corresponds now to a two-dimensional projection of the archetype associated with $\mathcal{K}_3^{(2)}$. The kernel may be defined by the two independent cycles with zero net voltage, namely $e_1e_2e_4$ and $e_3e_6e_5$. The kernel of the projection is described by matrix K as follows (notice the first two rows corresponding to the above referred cycles), leading to the projection matrix P,

$$\mathsf{K} = \begin{pmatrix} 1 & 1 & 0 & 1 & 0 & 0 \\ 0 & 0 & 1 & 0 & 1 & 1 \\ 1 & 0 & \overline{1} & \overline{1} & 0 & 1 \\ \overline{1} & 1 & 0 & 0 & 1 & \overline{1} \end{pmatrix},$$

$$\mathsf{P} = \begin{pmatrix} 1/3 & 1/6 & -1/6 & 1/6 & -1/6 & 1/3 \\ 1/6 & 1/3 & -1/6 & 1/6 & 1/3 & -1/6 \\ -1/6 & -1/6 & 1/3 & 1/3 & 1/6 & 1/6 \\ 1/6 & 1/6 & 1/3 & 1/3 & -1/6 & -1/6 \\ -1/6 & 1/3 & 1/6 & -1/6 & 1/3 & 1/6 \\ 1/3 & -1/6 & 1/6 & -1/6 & 1/6 & 1/3 \end{pmatrix}.$$

Only two cycles are now needed to define the basis of the embedding and these are listed as rows of matrix L, leading to the metric tensor Z,

$$\mathsf{L} = \begin{pmatrix} 1 & 0 & 0 & 0 & 0 & \overline{1} \\ 0 & 0 & \overline{1} & 1 & 0 & 0 \end{pmatrix},$$

$$\mathsf{Z} = \begin{pmatrix} 4/3 & -2/3 \\ -2/3 & 4/3 \end{pmatrix}.$$

The cycle–co-cycle matrix is clearly the same as that of the **qtz** net; only the voltage matrix needs to be written to obtain the arc matrix,

$$\alpha(\mathsf{B}) = \begin{pmatrix} 1 & 0 \\ \overline{1} & \overline{1} \\ 0 & -1 \\ 0 & 1 \\ 0 & 0 \\ 0 & 0 \end{pmatrix}, \quad \Omega^+ = \begin{pmatrix} 1/2 & 0 \\ -1/2 & -1/2 \\ 0 & -1/2 \\ 0 & 1/2 \\ 1/2 & 1/2 \\ -1/2 & 0 \end{pmatrix}.$$

If we set point *A* at position (1/2, 1/2), we obtain the following coordinates, corresponding to Wyckoff position 3*c* in space-group type *p6mm*,

$$\begin{cases} A: & 1/2, & 1/2, \\ B: & 0, & 1/2, \\ C: & 1/2, & 0. \end{cases}$$

8.4. The *β*-*W* net

We look at another two-dimensional net called *β*-*W* (vertex symbol $[3.6.3.6][3.3.6.6]^2$), also admitting $\mathcal{K}_3^{(2)}$ as its quotient graph, as given in Fig. 10.

We may again find two independent cycles with zero net voltage, namely $e_1e_2e_3$ and $e_3e_6e_5$. Note that these cycles run along a common edge, e_3, whereas the two cycles defining the kernel for **kgm** are edge-disjoint. The kernel of the projection is then described by matrix K as follows (notice the first two rows corresponding to the above referred cycles), leading to the projection matrix P,

$$\mathsf{K} = \begin{pmatrix} 1 & 1 & 1 & 0 & 0 & 0 \\ 0 & 0 & 1 & 0 & 1 & 1 \\ 1 & 0 & \overline{1} & \overline{1} & 0 & 1 \\ \overline{1} & 1 & 0 & 0 & 1 & \overline{1} \end{pmatrix},$$

$$\mathsf{P} = \begin{pmatrix} 7/24 & -5/24 & -1/12 & 1/6 & 7/24 & -5/24 \\ -5/24 & 7/24 & -1/12 & 1/6 & -5/24 & 7/24 \\ -1/12 & -1/12 & 1/6 & -1/3 & -1/12 & -1/12 \\ 1/6 & 1/6 & -1/3 & 2/3 & 1/6 & 1/6 \\ 7/24 & -5/24 & -1/12 & 1/6 & 7/24 & -5/24 \\ -5/24 & 7/24 & -1/12 & 1/6 & -5/24 & 7/24 \end{pmatrix}.$$

The lattice basis of the embedding in the edge space is the same as for **kgm** and leads to the following metric tensor,

$$\mathsf{Z} = \begin{pmatrix} 1 & 0 \\ 0 & 3/2 \end{pmatrix}.$$

The cycle–co-cycle matrix is still the same as that of the **qtz** net, so we just write the voltage matrix and derive the arc matrix,

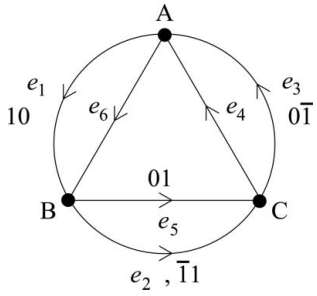

Figure 10
The labelled quotient graph of the β-W net.

$$\alpha(\mathsf{B}) = \begin{pmatrix} 1 & 0 \\ \overline{1} & 0 \\ 0 & -1 \\ 0 & 1 \\ 0 & 0 \\ 0 & 0 \end{pmatrix}, \quad \Omega^{+} = \begin{pmatrix} 1/2 & 1/6 \\ -1/2 & 1/6 \\ 0 & -1/3 \\ 0 & 2/3 \\ 1/2 & 1/6 \\ -1/2 & 1/6 \end{pmatrix}.$$

If we set point A at position $(1/2, 1/3)$, we obtain the following coordinates, corresponding to Wyckoff positions $2h$ for A and C and $1b$ for B in space-group type $p2mm$,

$$\begin{cases} A: & 1/2, & 1/3, \\ B: & 0, & 1/2, \\ C: & 1/2, & 2/3. \end{cases}$$

The derived embedding of the β-W net is represented in Fig. 11 with the rectangular unit cell highlighted. Although the space group of the embedding is maximal, it is clear that more regular embeddings can be drawn by asking, for example, that all six arcs be embedded with the same length. We examine the possibility of realizing such new constraints within the maximal space group in the following section.

9. Non-barycentric embeddings of stable nets

We shall consider two examples of non-barycentric embeddings of stable nets in this section. In the first one, the coordinates and lattice vectors of the barycentric embedding are simply altered to obtain a better embedding within the same space-group type. In the second example, we allow a reduction in the symmetry of the embedding, as it occurs in real crystal structures. In both examples, the embedding is obtained using equation (1), with Corollary 7.1 ensuring that the maximum symmetry is attained.

9.1. A regular embedding of the β-W net

The projection method provides a Euclidian embedding of any crystallographic net with maximum symmetry but with strongly constrained geometry. It may be noted that continuous distortions of the embedding enable, in some cases, its geometrical properties to be changed within the same space-group type. From Proposition 5.1, two different modes of distortion can be considered; one may change the lattice parameters of the archetypical embedding and/or shift some vertex lattices from their barycentric position. The former

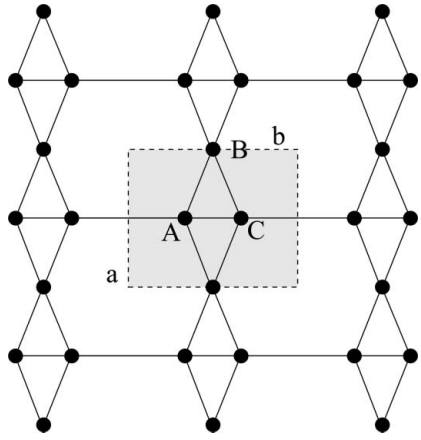

Figure 11
Archetypical embedding of the β-W net.

mode depends on the number of freedom degrees left by the metric tensor. In cubic groups, for instance, the length ratios cannot be changed. In the latter mode, the vectors of the co-cycle basis should be projected onto a set of non-zero vectors globally invariant by the point-group operations of the embedding. Site symmetry imposes strong restrictions to possible values of shift vectors. We analyse in detail the case of the β-W net.

From the arc matrix shown above, the lengths of arcs e_3 and e_4 are, respectively, one third and two thirds of lattice parameter b. Hence, no modification of lattice parameters can change the length ratio between these two arcs. Now, vertex B is located on Wyckoff site $1b$ of local symmetry $2mm$; no shift can preserve this symmetry. On the other hand, vertices A and C are situated on a mirror plane (site symmetry m) so that any shift along the direction of the plane is allowed. Naturally, the two shift vectors on A and C must be related by symmetry since the two point lattices are images of each other by reflection. But this condition is automatically fulfilled since the sum of the outgoing arcs on the complete set of vertices is zero. We may thus change the voltage matrix $\alpha(\mathsf{B})$ as follows and obtain the more general arc matrix $\Omega^{+}(x)$ (note the projection of the first co-cycle basis vector on $0x$),

$$\alpha(\mathsf{B}) = \begin{pmatrix} 1 & 0 \\ \overline{1} & 0 \\ 0 & -1 \\ 0 & 1 \\ 0 & x \\ 0 & 0 \end{pmatrix}, \quad \Omega^{+}(x) = \begin{pmatrix} 1/2 & 1/6 + x/6 \\ -1/2 & 1/6 + x/6 \\ 0 & -1/3 - x/3 \\ 0 & 2/3 - x/3 \\ 1/2 & 1/6 + x/6 \\ -1/2 & 1/6 + x/6 \end{pmatrix}.$$

Equalling the lengths of e_3 and e_4 gives $x = 1/2$, with the following new arc matrix and corresponding fractional coordinates,

$$\Omega^{+}(1/2) = \begin{pmatrix} 1/2 & 1/4 \\ -1/2 & 1/4 \\ 0 & -1/2 \\ 0 & 1/2 \\ 1/2 & 1/4 \\ -1/2 & 1/4 \end{pmatrix}, \quad \begin{cases} A: & 1/2, & 1/4, \\ B: & 0, & 1/2, \\ C: & 1/2, & 3/4. \end{cases}$$

It is clear that we can still define lattice parameters in space-group type $p2mm$ to obtain all six arcs of unit length, by choosing $a = \sqrt{3}$ and $b = 2$.

9.2. α-Cristobalite

Fig. 12 shows the labelled quotient graph, $\mathcal{C}_4^{(2)}$ (the 4-cycle with double edges), of the net associated with α-cristobalite taken with relation to the experimental translation group T ($Z = 4$), according to Peacor (1973). The unit cell is twice that of β-cristobalite ($Z = 2$), but α- and β-cristobalite are structurally isomorphic and the associated net is isomorphic to diamond (**dia**). If we use the information contained in the quotient graph, the *SYSTRE* program will provide the ideal embedding with space group $Fd\bar{3}m$ and identify the net as **dia**. In the same way, the projection method described above will give the ideal coordinates of the barycentric embedding, which are those of β-cristobalite. This will happen because the fixed-point free automorphism

$$\varphi = (A, C)(B, D)(e_1, e_3)(e_2, e_4)(e_5, \bar{e}_8)(e_6, \bar{e}_7)$$

of the labelled quotient graph does not change the net voltage over any cycle, so that it describes a combinatorial translation of the net, which in turn generates a translation of the barycentric embedding. It may be verified that the quotient of $\mathcal{C}_4^{(2)}$ by φ is isomorphic to $\mathcal{K}_2^{(4)}$, the quotient graph of **dia**. In order to obtain the correct information from the effective (experimental) quotient graph, we need to introduce some distortion in the unit cell according to the symmetry lowering. This can only be done by choosing different co-lattice vectors for the co-cycles at vertices A and C, and/or B and D, which will break the ideal symmetry. Moreover, the experimental translation subgroup T is not a normal subgroup of the full automorphism group of the net. Indeed, there is no automorphism of order 3 in $\mathcal{C}_4^{(2)}$, so that no threefold rotation in the net **dia** can respect the translational equivalence classes by T. Hence, we shall determine the ideal point group of α-cristobalite from a maximal subgroup of $\mathrm{Aut}(\mathcal{C}_4^{(2)})$ that exchanges the cycle vectors of zero net voltage and does not contain φ. The co-lattice vectors will then be chosen according to this point group.

We first determine the ideal metric tensor according to the labelled quotient graph. We begin with the kernel and lattice matrices K and L,

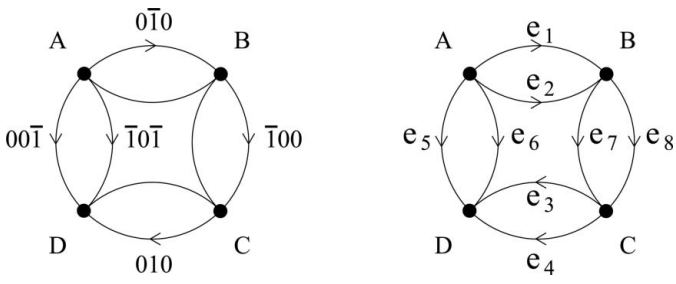

Figure 12
Voltage graph of α-cristobalite, with edges labelled on the right.

$$\mathsf{K} = \begin{pmatrix} 1 & \bar{1} & \bar{1} & 1 & 0 & 0 & 0 & 0 \\ 0 & 0 & 0 & 0 & 1 & \bar{1} & \bar{1} & 1 \\ 1 & 1 & 0 & 0 & 1 & 1 & 0 & 0 \\ 0 & 0 & 1 & 1 & 1 & 1 & 0 & 0 \\ 0 & 0 & 1 & 1 & 0 & 0 & \bar{1} & \bar{1} \end{pmatrix},$$

$$\mathsf{L} = \begin{pmatrix} 0 & 0 & 0 & 0 & 0 & 0 & 1 & \bar{1} \\ \bar{1} & 1 & 0 & 0 & 0 & 0 & 0 & 0 \\ 0 & 1 & 1 & 0 & \bar{1} & 0 & 1 & 0 \end{pmatrix},$$

$$\mathsf{Z} = \begin{pmatrix} 1 & 0 & 0 \\ 0 & 1 & 0 \\ 0 & 0 & 2 \end{pmatrix}.$$

As expected, the metric tensor indicates a primitive tetragonal cell. We shall now build a linear representation, Γ, of the automorphisms of $\mathcal{C}_4^{(2)}$ using the lattice basis of α-cristobalite. Consider, for example, the images of three cycle vectors with independent net voltages 100, 010 and 001 by the automorphism

$$\theta = (A, B, C, D)(e_1, e_7, e_4, \bar{e}_5)(e_2, e_8, e_3, \bar{e}_6).$$

We may choose, respectively, the cycles $(e_5 - e_6)$, $(e_2 - e_1)$ and $(e_2 + e_7 + e_3 - e_5)$. We initially form the images of these cycles by θ and then read the net voltages over the image cycles,

$$\begin{cases} (e_5 - e_6) & \rightarrow & (-e_1 + e_2) & : & 010, \\ (e_2 - e_1) & \rightarrow & (e_8 - e_7) & : & \bar{1}00, \\ (e_2 + e_7 + e_3 - e_5) & \rightarrow & (e_8 + e_4 - e_6 + e_1) & : & 001, \end{cases}$$

from which we write the associated matrix

$$\Gamma(\theta) = \begin{pmatrix} 0 & \bar{1} & 0 \\ 1 & 0 & 0 \\ 0 & 0 & 1 \end{pmatrix}.$$

Since this matrix corresponds to a fourfold rotation of the lattice, we look for a maximal acceptable subgroup of $\mathrm{Aut}(\mathcal{C}_4^{(2)})$ that contains θ. $\mathrm{Aut}(\mathcal{C}_4^{(2)})$ is the direct product of $\mathrm{Aut}(\mathcal{C}_4)$ by the group of order 2^4 that exchanges the four double edges. But we observe that the cycles $(e_5 - e_6)$ and $(e_7 - e_8)$ have the same net voltage 100. In the same way, $(e_2 - e_1)$ and $(e_4 - e_3)$ have net voltage 010. Each pair of cycles must therefore exchange together, restricting possible permutations to the products $(e_1, e_2)(e_3, e_4)$ and $(e_5, e_6)(e_7, e_8)$. Moreover, it is easily verified that, in combination with θ, these products generate the undesirable automorphism φ as follows,

$$\begin{aligned} \{\theta(e_1, e_2)(e_3, e_4)\}^2 &= \{\theta(e_5, e_6)(e_7, e_8)\}^2 \\ &= \theta^2(e_1, e_2)(e_3, e_4)(e_5, e_6)(e_7, e_8) \\ &= \varphi. \end{aligned}$$

Automorphisms corresponding to double edge exchanges must therefore be rejected and the symmetry point group of α-cristobalite is isomorphic to $\mathrm{Aut}(\mathcal{C}_4)$. There are, however, two possible edge permutations associated with vertex permutation (A, C) and satisfying the above constraints, namely

$$\begin{cases} \varepsilon_1 = (A, C)(e_1, \overline{e}_8)(e_2, \overline{e}_7)(e_3, e_5)(e_4, e_6), \\ \varepsilon_2 = (A, C)(e_1, \overline{e}_7)(e_2, \overline{e}_8)(e_3, e_6)(e_4, e_5), \end{cases}$$

with linear representations in the lattice basis

$$\Gamma(\varepsilon_1) = \begin{pmatrix} 0 & \overline{1} & 0 \\ \overline{1} & 0 & 0 \\ 0 & 0 & \overline{1} \end{pmatrix}, \quad \Gamma(\varepsilon_2) = \begin{pmatrix} 0 & 1 & 0 \\ 1 & 0 & 0 \\ 0 & 0 & 1 \end{pmatrix}.$$

It may be checked that the two linear representations of the subgroups $G_1 = \langle \varepsilon_1, \theta \rangle$ and $G_2 = \langle \varepsilon_2, \theta \rangle$ generated by any of these permutations together with the automorphism θ define the same geometric crystal class 422. We may now determine the exact nature of the isometry generated by these automorphisms by looking at their translation part. Consider, for example, the automorphism in the net, which is obtained by lifting θ, and maps some vertex A_0 in (translational) class A to a vertex B_0 in class B with A_0B_0 lifted from e_1. On a second application of this same automorphism, edge e_1 is sent to e_7 by θ and vertex B_0 to some vertex C_0 in class C. Therefore, as a net result of the two consecutive mappings, the first vertex A_0 has been sent to vertex C_0 associated with the path $AC = e_1 + e_7$. Repeating this process four times, we see that vertex A_0 is mapped to some vertex A_1 in the same class, but the path A_0A_1 is lifted from the cycle $e_1 + e_7 + e_4 - e_5$ with net voltage 001. This shows that the associated isometry is a fourfold screw rotation with screw vector [001]/4. On the other hand, ε_1 and ε_2 have each two fixed vertices, hence must correspond to a twofold rotation with axis $[1\overline{1}0]$ and [110], respectively. The two groups may be distinguished by analysing the combinations $\theta\varepsilon_1$ and $\theta\varepsilon_2$,

$$\begin{cases} \theta\varepsilon_1 = (A, D)(B, C)(e_1, \overline{e}_3)(e_2, \overline{e}_4)(e_5, \overline{e}_6)(e_7, \overline{e}_8), \\ \theta\varepsilon_2 = (A, D)(B, C)(e_1, \overline{e}_4)(e_2, \overline{e}_3)(e_5, \overline{e}_5)(e_6, \overline{e}_6)(e_7, \overline{e}_7)(e_8, \overline{e}_8), \end{cases}$$

with linear representation

$$\Gamma(\theta\varepsilon_1) = \begin{pmatrix} 1 & 0 & 0 \\ 0 & \overline{1} & 0 \\ 0 & 0 & \overline{1} \end{pmatrix}, \quad \Gamma(\theta\varepsilon_2) = \begin{pmatrix} \overline{1} & 0 & 0 \\ 0 & 1 & 0 \\ 0 & 0 & \overline{1} \end{pmatrix}.$$

On proceeding as above, it may be verified that $\theta\varepsilon_1$ determines a twofold screw rotation with screw vector [100]/2 while $\theta\varepsilon_2$ determines a twofold rotation with axis [010]. Hence, G_1 leads to space-group type $P4_12_12$ (No. 92) and G_2 to space-group type $P4_122$ (No. 91).

We now determine the distortion that effectively realizes the symmetry reduction. Let us call $L_A^*, \ldots, L_D^*$ the co-lattice vectors at vertices $A, \ldots, D$. We only need one of them since they are related by the fourfold rotation. Moreover, they should respect site symmetries. Hence, L_B^* is along the rotation axis associated with automorphism ε_i,

$$\begin{cases} i = 1 : L_B^* = x\overline{x}0, \\ i = 2 : L_B^* = xx0, \end{cases}$$

where x is a distortion parameter.

The two possibilities are shown in Fig. 13. It appears that the first one, associated with space group $P4_12_12$, should be preferred, in agreement with experimental data. It corresponds to an angular distortion of the silicon coordination polyhedron and does not alter bond lengths significantly. On the contrary, distortion along space group $P4_122$ alternately shortens and lengthens the bonds, a situation which may not be so favourable in the energetic viewpoint. Accordingly, it may be observed that all edges of the quotient graph are equivalent by G_1 while they form two orbits by G_2.

It remains to calculate the atomic coordinates according to equation (1),

$$\mathsf{B}^* = \begin{pmatrix} 1 & \overline{1} & 0 & 0 & 0 & 0 & 0 & 0 \\ 0 & 0 & 1 & \overline{1} & 0 & 0 & 0 & 0 \\ 0 & 0 & 0 & 0 & 1 & \overline{1} & 0 & 0 \\ 0 & 0 & 0 & 0 & 0 & 0 & 1 & \overline{1} \\ 0 & 1 & 1 & 0 & \overline{1} & 0 & 1 & 0 \\ 1 & 1 & 0 & 0 & 1 & 1 & 0 & 0 \\ \overline{1} & \overline{1} & 0 & 0 & 0 & 0 & 1 & 1 \\ 0 & 0 & 1 & 1 & 0 & 0 & \overline{1} & \overline{1} \end{pmatrix}, \quad \alpha(\mathsf{B}) = \begin{pmatrix} 0 & \overline{1} & 0 \\ 0 & \overline{1} & 0 \\ 1 & 0 & 0 \\ 1 & 0 & 0 \\ 0 & 0 & 1 \\ \overline{x} & \overline{x} & 0 \\ x & \overline{x} & 0 \\ x & x & 0 \end{pmatrix},$$

where the last three rows correspond to the co-lattice vectors L_A^*, L_B^* and L_C^*,

$$\Omega^+(x) = \begin{pmatrix} \overline{x}/2 & \overline{1}/2 & 1/4 \\ \overline{x}/2 & 1/2 & 1/4 \\ x/2 & \overline{1}/2 & 1/4 \\ x/2 & 1/2 & 1/4 \\ 1/2 & \overline{x}/2 & \overline{1}/4 \\ \overline{1}/2 & \overline{x}/2 & \overline{1}/4 \\ 1/2 & \overline{x}/2 & 1/4 \\ \overline{1}/2 & \overline{x}/2 & 1/4 \end{pmatrix}.$$

If we set point A as follows, we obtain the coordinates of the three other points,

$$\begin{cases} A: & 1/4 + x/4 & 1/4 + x/4 & 0, \\ B: & 1/4 - x/4 & 3/4 + x/4 & 1/4, \\ C: & 3/4 - x/4 & 3/4 - x/4 & 1/2, \\ D: & 3/4 + x/4 & 1/4 - x/4 & 3/4, \end{cases}$$

which are in agreement with Wyckoff position 4*a* at $1/4 + x/4, 1/4 + x/4, 0$ in space group $P4_12_12$. Comparing with experimental data, we obtain the distortion parameter $x \simeq 0.2$ [Si coordinates are at 0.3002, 0.3002, 0 at 301 K according to Peacor (1973)].

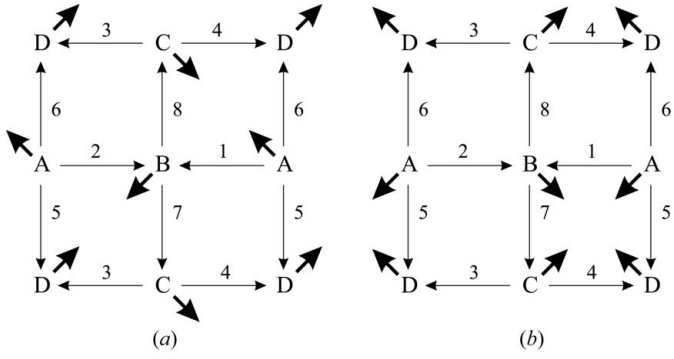

Figure 13
Two possible sets of symmetry-lowering co-lattice vectors in β-cristobalite, seen in projection along the 001 axis of α-cristobalite: from $Fd\overline{3}m$ to (*a*) $P4_12_12$, (*b*) $P4_122$.

10. Embeddings of unstable 3-periodic minimal nets

Some crystallographic nets may derive from a graph with bridges, as the 2-periodic net shown in Fig. 5; it is also the case for seven of the 3-periodic minimal nets (Beukemann & Klee, 1992). Because bridges belong to the co-cycle space of the quotient graph, any barycentric representation of the net presents collisions. It is the aim of this section to propose a non-barycentric embedding of maximum symmetry for each of these nets. The labelled quotient graphs are gathered in Fig. 14, where the nets have been named according to the nomenclature given in the above-cited paper. The argument will parallel that of the previous section. Quotient graphs G of 3-periodic minimal nets do not possess any non-trivial cycle vector of zero net voltage. Hence, the point group of the embedding should be a maximal subgroup of the point group derived from Aut(G), which exchanges the co-lattice vectors and avoids collisions. According to Corollary 7.1, the embedding provided by equation (1) will belong to the appropriate space group. For each net, determination of the space group and definition of the co-cycle vectors are briefly described. Cell parameters and atomic coordinates are displayed in Table 1. Because it is most probable that loops in the quotient represent complex links in a crystal structure, organic ligands for example, they have been arbitrarily embedded as lines of length 3. Unless otherwise specified, other edges have unit length.

Table 1
Embeddings of unstable 3-periodic minimal nets.

Net	Space group	Lattice parameters	Point coordinates
2(3, 5)2	*C*2*mm*	$a = 3$	*A*: 0, 0, 0
		$b = 3\sqrt{3}$	*B*: 1/3, 0, 0
		$c = 3$	
3(3^2, 4)2	*C*2*mm*	$a = 3$	*C*: 0, 0, 0
		$b = \sqrt{3}$	*B*: 1/3, 0, 0
		$c = 3$	*A*: 2/3, 0, 0
3(3^2, 4)4	*C*121	$a = b = 3\sqrt{2}$	*C*: 0, 0, 0
		$c = 3$	*A*: 0.172, −0.172, 0.15
		$\beta = 114^\circ$	
3(3^2, 4)5	*Pmm*2	$a = 2$	*A*: 0, 0, 0
		$b = c = 3$	*B*: 1/2, 0, 0
			C: 1/2, 0, 1/3
4(3)3	*C*2*mm*	$a = \sqrt{15}$	*A*: 0, 0, 0
		$b = 5$	*B*: 0, 1/5, 0
		$c = 3$	*D*: $1/\sqrt{15}$, 0, 0
4(3)4	*R*32	$a = 3$	*D*: 0, 0, 0
		$\alpha = 83.6^\circ$	*A*: 0, 1/4, 3/4
4(3)5	*C*2*cm*	$a = b = 3\sqrt{2}$	*B*: 0, $\sqrt{2}/24$, −1/4
		$c = \sqrt{3}$	*A*: 0, $5\sqrt{2}/24$, −1/4

10.1. Net 2(3, 5)2

The automorphism group of the graph is generated by the permutations $(e_1, \overline{e}_1)$ and (e_1, e_2) of the two equivalent loops at vertex A together with the inversion $(e_3, \overline{e}_3)$ of the loop at vertex B. The group has order 16 and is isomorphic to point group 4/*mmm*, the only point group of this order. Edge AB generates the co-cycle space and hence should be embedded as the unique co-lattice vector. Being unique it must be invariant by every point-group symmetry operation of the embedding. The fourfold rotation cannot be retained because it would lead to superposition of line AB with the **c** axis. The co-lattice vector must be along a twofold axis and contained in reflection planes, so we are left with *mm*2 as the maximal acceptable subgroup of 4/*mmm*. This subgroup is generated by the permutations $(e_1, e_2)(e_3, \overline{e}_3)$ and $(e_3, \overline{e}_3)$ corresponding to the twofold rotation with axis 110 (in the primitive cell) and vertical reflection, respectively. The net belongs to space-group type *C*2*mm* (No. 38). The edge AB must therefore be embedded as the co-lattice vector along 100 of the centred cell. Cell parameters have been chosen in order to have a minimum angle of 60° between lines at point A.

10.2. Net 3(3^2, 4)2

The automorphism group of the graph is generated by the permutations (e_1, e_2), (e_1, e_2, e_3) and the inversion $(e_5, \overline{e}_5)$. The three transpositions (e_1, e_2), (e_1, e_3) and (e_2, e_3) generate three reflection symmetries in a same conjugacy class while the inversion $(e_5, \overline{e}_5)$ generates a fourth independent reflection. With four reflection operations and order 12, the point group of the net is $\overline{6}2m$. As above, the edge BC should be embedded as a co-lattice vector which is invariant by any point-group operation. Threefold rotations would yield superposition with the **c** axis and must be discarded. These constraints leave again

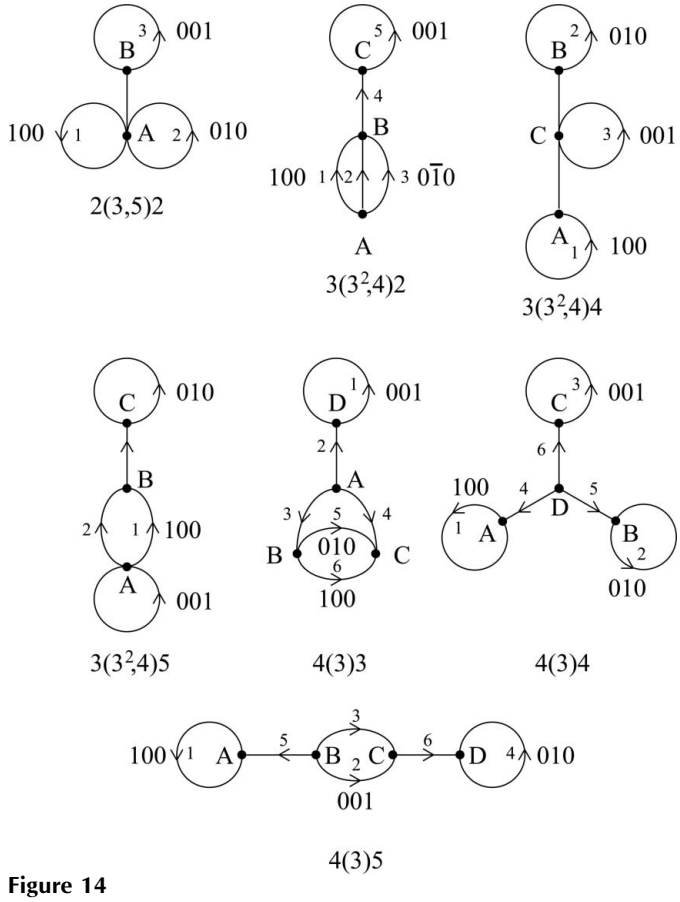

Figure 14
The labelled quotient graphs of the seven 3-periodic minimal nets; edges are labelled by numerals.

*mm*2 as the maximal acceptable subgroup with, for example, the *m* operations generated by (e_1, e_2) and $(e_5, \overline{e}_5)$ (space group *C*2*mm*, No. 38). On writing the corresponding linear representations, it may be verified that the common axis is along 120, which enables the arc matrix to be written as follows (note the zero co-lattice vector at vertex *A*),

$$\mathsf{B}^* = \begin{pmatrix} 1 & \overline{1} & 0 & 0 & 0 \\ 0 & 1 & \overline{1} & 0 & 0 \\ 0 & 0 & 0 & 0 & 1 \\ 1 & 1 & 1 & 0 & 0 \\ 0 & 0 & 0 & \overline{1} & 0 \end{pmatrix}, \quad \alpha(\mathsf{B}) = \begin{pmatrix} 1 & 0 & 0 \\ 0 & 1 & 0 \\ 0 & 0 & 1 \\ 0 & 0 & 0 \\ x & 2x & 0 \end{pmatrix},$$

$$\Omega^+(x) = \begin{pmatrix} 2/3 & 1/3 & 0 \\ -1/3 & 1/3 & 0 \\ -1/3 & -2/3 & 0 \\ -x & -2x & 0 \\ 0 & 0 & 1 \end{pmatrix}.$$

10.3. Net 3(3², 4)4

The automorphism group of the graph is generated by the permutation (e_1, e_2) of the two loops at vertices *A* and *B* and by the inversion of each of the three loops. Having order 16, it is isomorphic to 4/*mmm*. In order to avoid crossings, one can only retain the twofold rotation generated by permutation $(A, B)(1, 2)(3, \overline{3})$ so that the point group is 2. The space group is then *C*2 (*C*121, No. 5).

10.4. Net 3(3², 4)5

The automorphism group of the graph is generated by the permutation (e_1, e_2) and by the inversion of the two loops at vertices *A* and *C*; it is isomorphic to point group *mmm*. The only subgroup avoiding crossings is *mm*2, which is derived from the inversion of the two loops and the bridge *BC* is along the twofold rotation axis, parallel to 001. The space group is *Pmm*2 (No. 25).

10.5. Net 4(3)3

The automorphism group of the graph is generated by the permutations (e_5, e_6), $(e_3, e_4)(e_5, \overline{e}_6)$ and by the inversion of the loop e_1 at vertex *D*. It is also isomorphic to point group *mmm* and the only subgroup avoiding crossings is *mm*2, which is derived from the loop inversion and permutation $(e_3, e_4)(e_5, \overline{e}_6)$. The bridge *AD* is along the twofold rotation axis, parallel to $1\overline{1}0$. The space group is *C*2*mm* (No. 38) and atomic coordinates are obtained from equation (1),

$$\mathsf{B}^* = \begin{pmatrix} 1 & 0 & 0 & 0 & 0 & 0 \\ 0 & 0 & 1 & \overline{1} & 1 & 0 \\ 0 & 0 & 1 & \overline{1} & 0 & 1 \\ 0 & 1 & 0 & 0 & 0 & 0 \\ 0 & 0 & \overline{1} & 0 & 1 & 1 \\ 0 & 0 & 0 & 1 & 1 & 1 \end{pmatrix}, \quad \alpha(\mathsf{B}) = \begin{pmatrix} 0 & 0 & 1 \\ 0 & 1 & 0 \\ 1 & 0 & 0 \\ x & -x & 0 \\ 0 & 0 & 0 \\ 0 & 0 & 0 \end{pmatrix},$$

$$\Omega^+(x) = \begin{pmatrix} 0 & 0 & 1 \\ x & -x & 0 \\ 1/5 & 1/5 & 0 \\ -1/5 & -1/5 & 0 \\ -2/5 & 3/5 & 0 \\ 3/5 & -2/5 & 0 \end{pmatrix}.$$

Edges *BC* have been embedded as lines of length 2.

10.6. Net 4(3)4

The automorphism group of the graph is generated by the six permutations of the three vertices and the 2^3 inversions of the loops. With order 48, the point group of the net is thus $m\overline{3}m$. The maximal site symmetry one can embed the three edges incident to vertex *D* is $\overline{6}2m$. Two maximal acceptable common subgroups of $m\overline{3}m$ and $\overline{6}2m$ are 3*m* and 32. In both cases we may choose the threefold rotation of axis 111 derived from the permutation (e_1, e_2, e_3) as a first generator. Point group 3*m* is obtained by adding the reflection derived from (e_2, e_3) while 32 requires addition of the twofold rotation derived from $(e_1, \overline{e}_1)(e_2, \overline{e}_3)$ with axis along $01\overline{1}$. It may be verified that only 32 does not yield crossings. The space group is thus *R*32 (No. 155) and is obtained when edges e_4, e_5 and e_6 are embedded along $01\overline{1}$, $\overline{1}01$ and $1\overline{1}0$, respectively. Note that lines *AA* are along the 100 axis.

10.7. Net 4(3)5

The automorphism group of the graph is generated by the inversions of the loops at vertices *A* and *D* and the two permutations (e_2, e_3) and $(e_1, e_4)(e_2, \overline{e}_3)(e_5, e_6)$. With order 16, it is isomorphic to 4/*mmm*. The maximal subgroup avoiding crossings is generated by the two permutations (e_2, e_3) and $(e_1, e_4)(e_2, \overline{e}_3)(e_5, e_6)$ and is isomorphic to *mm*2. Note that the former permutation corresponds to a reflection in the horizontal plane and the latter corresponds to a glide reflection (if vertex *B* is first sent to $B + e_2$, a second mapping sends it to $B + e_2 - e_3 = B + \mathbf{c}$); the space group is *C*2*cm* (No. 40). Co-lattice vectors at vertices *B* and *C* may be taken equal to zero. Both equivalent edges e_5 and e_6 must then be embedded as co-lattice vectors along $1\overline{1}0$ (in the primitive cell) to obtain the right symmetry.

Whereas the space-group types found for the first six nets are in agreement with those given by Beukemann & Klee (1992), the maximum symmetry of the embedding of 4(3)5 is higher than that given by these authors (*Pm*, No. 6).

11. Embeddings of non-crystallographic nets

Equation (1) and Corollary 7.1 may also be applied in the case of non-crystallographic nets; it is thus possible to find embeddings whose symmetry operations are derived from the automorphisms of the quotient graph. It is known, however, that non-crystallographic nets admit more than one maximal translation group and the quotient graphs of the net by these translation groups are not necessarily isomorphic. In accordance to Definition 4.2, two maximal translation groups T_1 and T_2 of the net *N* determine two distinct periodic nets

(N, T_1) and (N, T_2) that may have non-isomorphic quotients and different embeddings of maximum symmetry. We shall illustrate our point on the 3-periodic net first described by Chung *et al.* (1984) obtained from the 1-periodic ladder, periodically repeated in two independent directions. Two labelled quotient graphs G_a and G_b of the net are given in Figs. 15(*a*) and 15(*b*), respectively; the reader may easily verify that the corresponding systre keys generate an error message from *SYSTRE*. The barycentric representations obtained from equation (1) effectively display collisions: edges e_1, e_6 and e_7 are embedded as the zero line, so that vertices A and B are embedded as the same point as well as vertices C, D and E. This result may be explained by considering the automorphism $\varphi = (e_2, e_5)(e_3, e_4)(e_6, e_7)(e_1, \overline{e}_1)$ of any of the quotient graphs. Because φ does not change any net voltage on cycle vectors in G ($G = G_a$ or G_b) it must generate a translation in the barycentric representation of the net. But E and F are fixed by φ, so that the corresponding isometry is the identity, with all its consequences. For instance, e_1 and its image $\overline{e}_1$ are embedded as the same line and must be the zero line, leading to a collision between A and B. To avoid collisions, we will use different co-lattice vectors at vertices A and B or C and D, making an obstacle to the translation. We shall determine these vectors by looking for the largest automorphism subgroup of Aut(G) that preserves the kernel $\mathcal{K}$ (the subspace of cycle vectors of zero net voltage) and does not contain φ.

We deal first with G_a. Besides φ, Aut(G_a) is generated by the inversion of the loop $(e_1, \overline{e}_1)$ and by the permutations (e_8, e_9), $(e_2, e_3)(e_4, e_5)$. The point group derived from the latter three automorphisms is *mmm*. It must be rejected because every point is located at a site of symmetry *mmm*, which implies that all co-lattice vectors are null. But we may take instead the subgroup generated by the product $\varphi(e_{10}, \overline{e}_{10})$ and by the permutations (e_8, e_9) and $(e_2, e_3)(e_4, e_5)$. The point group is still *mmm* but the co-lattice vectors at A and B, as well as C and D, are exchanged by the first permutation and should be along 100. This is in fact the only choice avoiding collisions. We may even choose $L^*_A = L^*_B = 0$ and $L^*_C = -L^*_D = x00$. The space group is *Pmmm* (No. 47); lattice parameters and coordinates providing lines of unit length, except along the 100 axis, are as follows ($x = 1/2$),

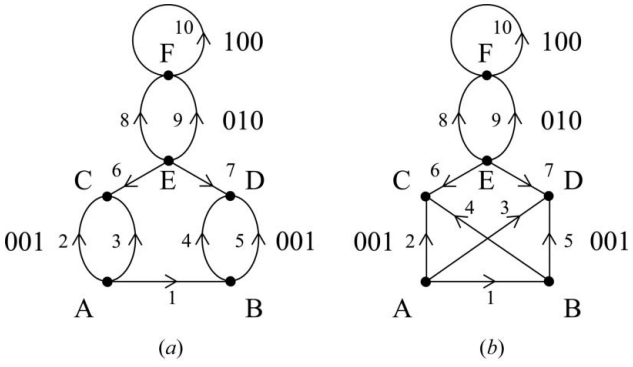

Figure 15
Two possible labelled quotient graphs of the same crystallographic net; edges are labelled by numerals.

$$\begin{cases} a = 4, \\ b = 2, \\ c = \sqrt{3}, \end{cases} \qquad \begin{cases} F: & 0 & 0 & 0, \\ E: & 0 & 1/2 & 0, \\ C: & 1/4 & 1/2 & 0, \\ A: & 1/8 & 1/2 & 1/2. \end{cases}$$

The argument is similar in the case of G_b, but it may be checked that most reflection symmetries produce crossings in the derived net. The largest possible point group is 222 generated by the following permutations,

$$\begin{cases} (e_2, e_5)(e_3, e_4)(e_6, e_7)(e_1, \overline{e}_1)(e_8, e_9)(e_{10}, \overline{e}_{10})(A, B)(C, D), \\ (e_2, e_4)(e_3, e_5)(e_8, e_9)(e_1, \overline{e}_1)(A, B). \end{cases}$$

The space group is $P222$ (No. 16). With C and D being invariant by the second automorphism, the corresponding co-lattice vectors are oriented along 100, the rotation axis. Similarly, co-lattice vectors at vertices A and B are along 010,

$$\begin{cases} L^*_C = -L^*_D = x00, \\ L^*_A = -L^*_B = 0y0. \end{cases}$$

Possible lattice parameters and coordinates are as follows (lines corresponding to edges e_2 to e_5 have length $\sqrt{2}$ for $x = y = 1$),

$$\begin{cases} a = 3, \\ b = 2, \\ c = \sqrt{3}, \end{cases} \qquad \begin{cases} F: & 0 & 0 & 0, \\ E: & 0 & 1/2 & 0, \\ C: & 1/3 & 1/2 & 0, \\ A: & 0 & 1/4 & 1/2. \end{cases}$$

Observe that the nets derived from G_a and G_b are isomorphic as nets, but not as periodic nets. Their maximum-symmetry embeddings belong to different space-group types and are not ambiently isotopic.

Supplementary materials provide an edge-definition file, drawings generated by *TOPOS* (Blatov, 2006) and the *TOPOS* database for the embeddings of the seven 3-periodic minimal nets with collision and the two non-crystallographic nets G_a and G_b.[1]

12. Summary and final considerations

Given a labelled quotient graph, it was shown that a Euclidian representation of the derived periodic net is completely determined, up to translation, by the choice of a lattice basis and of a co-lattice. Maximum-symmetry representations are obtained when the lattice belongs to the lattice type of the periodic net and the co-lattice is invariant by its point group. Barycentric representations, corresponding to the special case of an identically null co-lattice, automatically fulfil the latter condition. On the other hand, a periodic net with quotient graph G may be viewed as a quotient of the minimal net derived from G. These properties suggested considering the orthogonal projection of a barycentric embedding of the corresponding minimal net as a special construct with maximum symmetry. The lattice type of the net may be obtained directly from the metric tensor of this representation,

[1] Supplementary data for this article are available from the IUCr electronic archives (Reference: AU5105). Services for accessing these data are described at the back of the journal.

without previous knowledge of its space-group type. The projection itself is generally too much constrained and is not the best representation of the net. Equation (1) is preferentially used to obtain the fractional atomic coordinates. At this step, barycentric conditions may be relaxed and lower site symmetries imposed. Adequate lattice and distortion parameters may be chosen to obtain a refined embedding.

While the topology of a crystal structure is given by its labelled quotient graph, it is emphasized that the co-lattice vectors together with the lattice vectors provide a complete geometric descriptor of the structure. The co-lattice was interpreted as a measure of the distortion of the embedding in relation to the barycentric representation built on the same lattice. As such, a comparative analysis of co-lattice vectors from experimental data should provide valuable insights in questions of structural chemistry, in particular in the study of displacive transitions.

The author is grateful to W. E. Klee, J. S. Rutherford and D. M. Proserpio (Milan University) for fruitful discussions. D. M. Proserpio is also thanked for his help with *TOPOS*. CNPq, Conselho Nacional de Desenvolvimento e Pesquisa of Brazil, is acknowledged for support during the preparation of this work.

References

Beukemann, A. & Klee, W. E. (1992). *Z. Kristallogr.* **201**, 37–51.
Blatov, V. A. (2006). *IUCr CompComm Newsletter* **7**, 4–38. http://www.topos.ssu.samara.ru/.
Brown, H., Bülow, R., Neubüser, J., Wondratschek, H. & Zassenhaus, H. (1978). *Crystallographic Groups of Four-Dimensional Space.* New York: Wiley.
Chung, S. J., Hahn, Th. & Klee, W. E. (1984). *Acta Cryst.* A**40**, 42–50.
Delgado-Friedrichs, O. (2004). *Lecture Notes Comput. Sci.* **2912**, 178–189.
Delgado-Friedrichs, O. (2005). *Discrete Comput. Geom.* **33**, 67–81.
Delgado-Friedrichs, O., Foster, M. D., O'Keeffe, M., Proserpio, D. M., Treacy, M. M. J. & Yaghi, O. M. (2005). *J. Solid State Chem.* **178**, 2533–2554.
Delgado-Friedrichs, O. & O'Keeffe, M. (2003). *Acta Cryst.* A**59**, 351–360.
Delgado-Friedrichs, O. & O'Keeffe, M. (2005). *J. Solid State Chem.* **178**, 2480–2485.
Delgado-Friedrichs, O. & O'Keeffe, M. (2009). *Acta Cryst.* A**65**, 360–363.
Eon, J.-G. (1998). *J. Solid State Chem.* **138**, 55–65.
Eon, J.-G. (1999). *J. Solid State Chem.* **147**, 429–437.
Eon, J.-G. (2005). *Acta Cryst.* A**61**, 501–511.
Godsil, C. & Royle, G. (2004). *Algebraic Graph Theory*. New York: Springer.
Gross, J. L. & Tucker, T. W. (2001). *Topological Graph Theory*. New York: Dover.
Harary, F. (1972). *Graph Theory*. New York: Addison-Wesley.
Klee, W. E. (2004). *Cryst. Res. Technol.* **39**, 959–968.
Koch, E. & Fischer, W. (1978). *Z. Kristallogr.* **148**, 107–152.
O'Keeffe, M. & Hyde, B. G. (1980). *Philos. Trans. R. Soc. A*, **295**, 553–618.
O'Keeffe, M. & Peskov, M. A. & Ramsden, S. J. & Yaghi, O. M. (2008). *Acc. Chem. Res.* **41**, 1782–1789.
Peacor, D. R. (1973). *Z. Kristallogr.* **138**, 274–298.
Schwarzenberger, R. L. E. (1980). *N-Dimensional Crystallography*. London: Pitman.
Thimm, G. (2009). *Acta Cryst.* A**65**, 213–226.
Thimm, G. & Winkler, B. (2006). *Z. Kristallogr.* **221**, 749–758.
Wells, A. F. (1977). *Three-Dimensional Nets and Polyhedra.* New York: John Wiley and Sons.